Investigating a Link Between Topography and Scalloped Depressions in Utopia Planitia, Mars

by

Laurence A. Tognetti

A Thesis Presented in Partial Fulfillment
of the Requirements for the Degree
Master of Science

Approved April 2019 by the
Graduate Supervisory Committee

James F. Bell III, Chair
Mark S. Robinson
Kelin X. Whipple

ARIZONA STATE UNIVERSITY
May 2019

ABSTRACT

Western Utopia Planitia, located in the northern plains of Mars, is home to a myriad of possible periglacial landforms. One of these is scalloped depressions, defined primarily by their oval-shape and north-south asymmetry, including both pole-facing "steps" and an equator-facing slope. Scalloped depressions are thought to have formed through sublimation of ground ice in the Late Amazonian, consistent with the hypothesis that Mars is presently in an interglacial period marked by the poleward retreat of mid-latitudinal ice. The directional growth of scalloped depressions was mapped within the region and present a correlation between topography and scalloped depression development. It was determined that topography appears to play a role in scallop development, as noted by the most-densely scalloped region residing among a lower spatial density of craters previously mapped by *Harrison* et al. (2019). Within this region, scallops were also observed to be absent atop crater ejecta, but present atop crater ejecta in other regions of the study area. A large majority of scallops maintain a north-south asymmetry and observed changes in geomorphology that range from predominantly smoother terrain in the northern latitudes to very hummocky terrain dominated by possible periglacial features as latitude decreases. Mars Reconnaissance Orbiter (MRO) Context Camera (CTX) images were primarily used, with a few images coming from the MRO High Resolution Imaging Science Experiment (HiRISE). Observations are consistent with previous studies showing the overall density of scalloped depressions decreases with increasing latitude, with the majority exhibiting steps facing in a poleward direction. The majority of scallops observed to have steps in a non-poleward direction occur within in ice-rich regions mapped by *Stuurman* et al. (2016). It was ultimately

concluded that scallops demonstrating poleward-facing steps likely formed during periods of high obliquity on Mars in the Late Amazonian, while scallops within the ice-rich regions potentially formed at a greater range of obliquities.

This manuscript is dedicated to my Mother, Ann Buist Tognetti, who fueled my fascination with all things outer space. I wouldn't be in this field if not for her tireless dedication to allow me to dream about traveling among the stars and what kinds of life we might find out there. Thanks, Mom.

ACKNOWLEDGMENTS

I would like to thank Jim Bell for believing in me, and for Tanya Harrison for her patience in teaching me about Mars. The amount of knowledge I have gained about the Red Planet from both of these amazing individuals has been beyond rewarding. Thank you for taking a chance on me and thank you for the knowledge you have bestowed in me, as well.

TABLE OF CONTENTS

LIST OF FIGURES

Figure Page

Figure Page

LIST OF TABLES

Table Page

Chapter 1: Introduction

Utopia Planitia

Utopia Planitia is a basin in the northern hemisphere of Mars ~3300 km in diameter and centered at 49.7˚N, 118.0˚S (Figure 1). It was visited by the Viking 2 lander on September 3, 1976, touching down approximately 200 km west of the crater Mie at 48.269˚N, 225.990˚W.

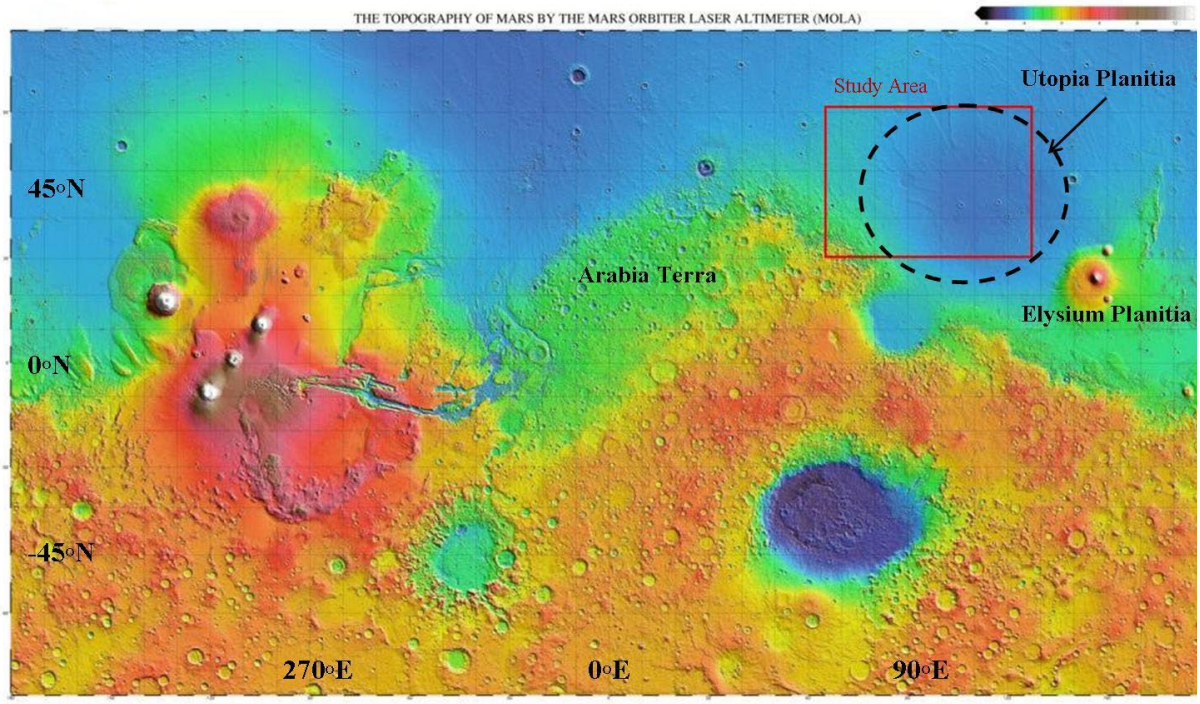

Figure 1: Utopia Planitia. Image from *Kerrigan* (2013).

Utopia Planitia exhibits a collection of landforms representing a variety of geomorphological surface processes, most notably rimless, shallow depressions, identified as “scalloped” depressions or “scallops” (*Lefort* et al., 2009), and other possible periglacial landforms such as polygons and pingo-like mounds (e.g., *Séjourné* et al., 2011) (Figure 2).

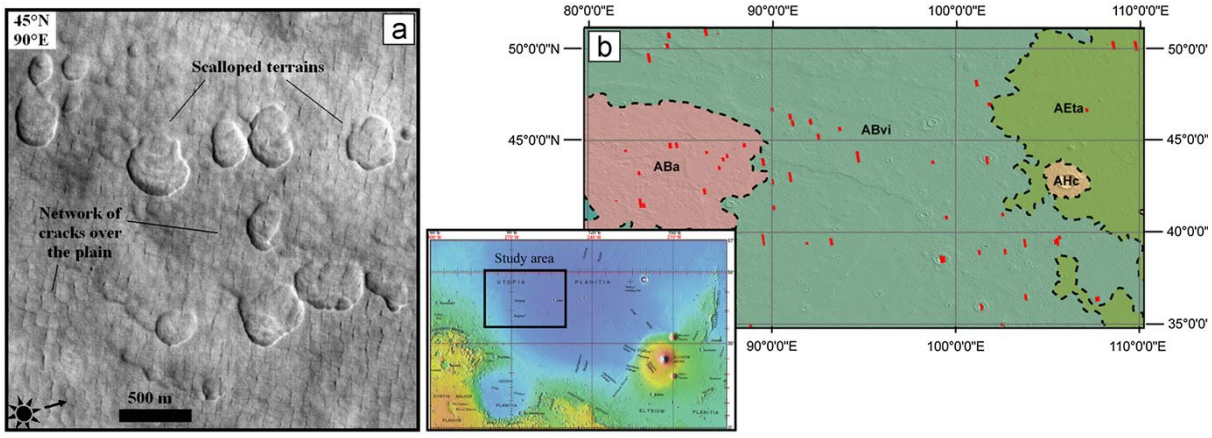

Figure 2: Periglacial landforms. Image from *Séjourné* et al. (2011).

The possible periglacial landforms on Mars mirror analog studies carried out in the Canadian Arctic (*Soare, Osinski, & Roehm,* 2008), Scandinavia (*Hauber, Reiss, & Ulrich*, 2011), Siberia (*Ulrich* et al., 2010), and Antarcticsa (*Levy, Head, & Marchant*, 2009). The study conducted by *Hauber* et al. (2011) in Scandinavia focused on the topographic analogue to martian crater interiors, establishing a correlation between periglacial landforms and the high relief present at crater walls.

While present-day Mars only allows for ice to be stable on the surface at the polar regions, the global distribution of water ice on Mars is affected in large part by obliquity variations. The obliquity of Mars has ranged from 13.6˚ to 46.9˚ over the past $10x10^6$ years over a 120 kyr cycle (*Laskar* et al., 2004). Changes in obliquity result in the redistribution of ice deposits between the poles and lower-latitude regions. Global Climate Model (GCM) results of *Levrard* et al. (2004) and *Madeleine* et al. (2009) predict that as obliquity decreases from high values of ~45˚, the low-latitude ice deposits become unstable and are redeposited in the mid-latitudes as an ice-dust deposit. As the

obliquity decreases further, this ice sublimates and is transported poleward via atmospheric circulation (*Levrard* et al., 2004).

Scalloped Depressions

Scalloped depressions have been proposed to originate from thermokarstic processes such as sublimation and and/or melting of near-surface ground ice (e.g., *Séjourné* et al., 2012). They are thought to populate western Utopia Planitia due to the ice-rich regolith that has undergone sublimation or thaw (*Stuurman* et al., 2016). Possible thermokarst features on Mars were first suggested from Mariner 9 images by *Sharp* (1973), which show similarities to terrestrial thermokarst terrains in Alaska that formed in unconsolidated sediments with variable ice content (*Gatto and Anderson*, 1975). *Morgenstern* et al. (2007) discussed how the size and shape of the depressions they studied in Utopia Planitia were very similar to terrestrial thermokarst depressions in NE Siberian ice-rich permafrost deposits. Although the possible meta-stability of highly-localized pockets of water on Mars today is acknowledged by many researchers (*Mellon and Jakosky*, 1993, 1995; *Schorghofer and Aharonson*, 2005; *Schorghofer*, 2007; *Hudson, Aharonson, and Schorghofer*, 2009; *Schorghofer and Forget*, 2012), very few of them believe that liquid water is/has been stable at the mid-latitudes of Utopia Planitia for a period of time sufficient to form the scalloped depressions by means of melting and evaporation.

Scalloped depressions on Mars typically form in material within smooth areas of mantling terrains, which may be the remnants of an ice-rich mid-latitude mantle that still covers the martian surface between ~30˚ and ~60˚ latitude (*Kreslavsky and Head*, 2003). A typical scalloped depression displays a gentle, equator-facing slope and a steeper, pole-

facing scarp, and a series of ridges, or “steps” interpreted to indicate direction of growth (e.g., (*Lefort* et al., 2009) (Figure 3).

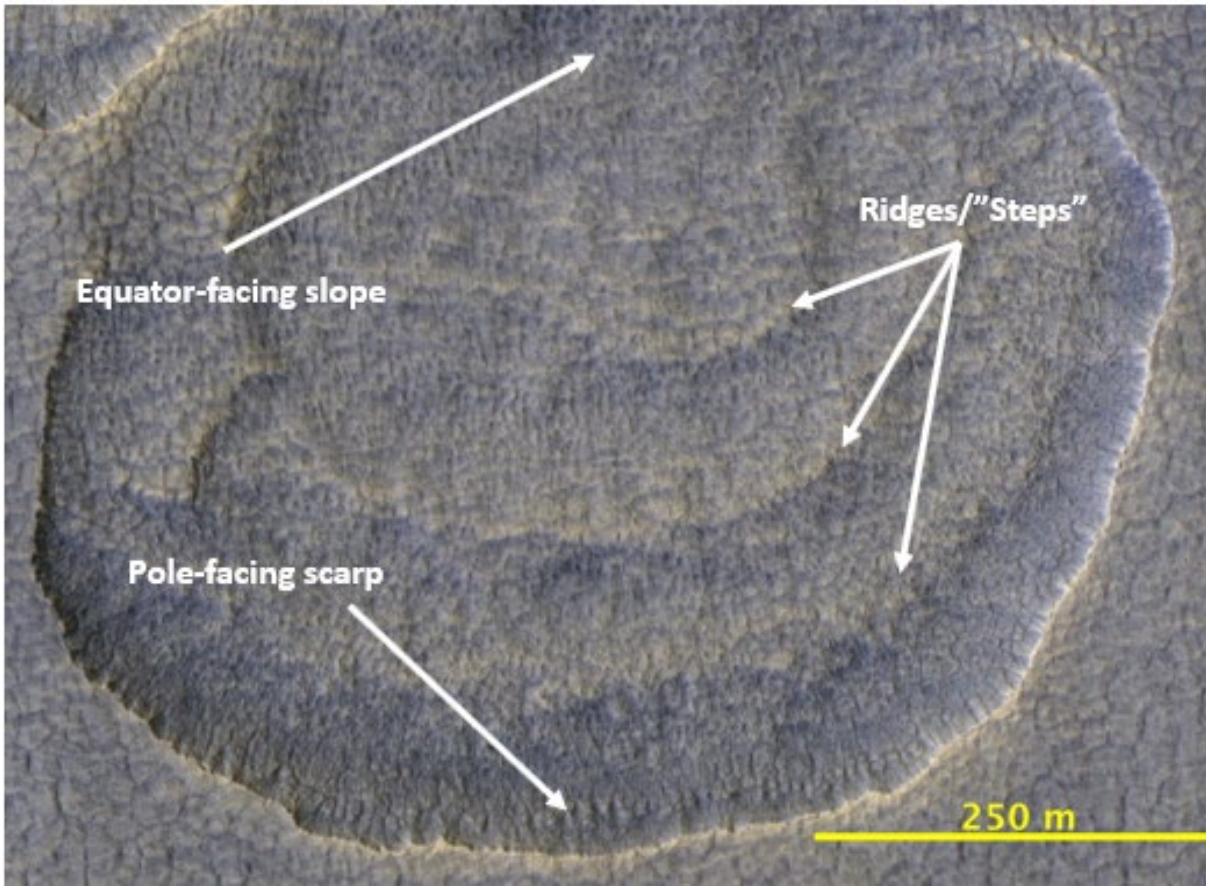

Figure 3: A typical scalloped depression (north is up and illumination is from the left in all figures unless otherwise noted; HiRISE ESP_027664_2245, 43.98˚N, 90.18˚E)

While the focus of this work is the identification of scalloped depressions strictly within Utopia Planitia, they have also been observed in the Peneus and Amphitrites regions, just south of Hellas Basin (Figure 4). These areas display a high concentration of polygonal terrains and scallop-shaped depressions reminiscent of periglacial landscapes on Earth (*Plescia*, 2003; *Lefort* et al., 2009; *Zanetti* et al., 2008). The scallops in these regions also display the similar physical characteristics in terms of possessing a pole-facing scarp and

equator-facing slope, with the exception that they appear to be growing towards the south pole.

Figure 4: Scalloped terrain in Peneus Patera. (HiRISE PSP_005698_1225, 57.0°S, 51.3°E, Ls = 330.6°). Image from *Lefort* et al. (2010).

Lefort et al. (2009) discovered a relationship between the scalloped depressions and interior polygons and ridges. They appear to evolve together, a process mainly influenced by sublimation, local proximity of ground ice to the surface, and obliquity variations (Figure 5). The polygons are thought to start off wide on flat terrain and progressively get thinner as the terrain sloped due to the formation of a scallop (Figure 6). This led to the conclusion that the polygons were older than the scallops.

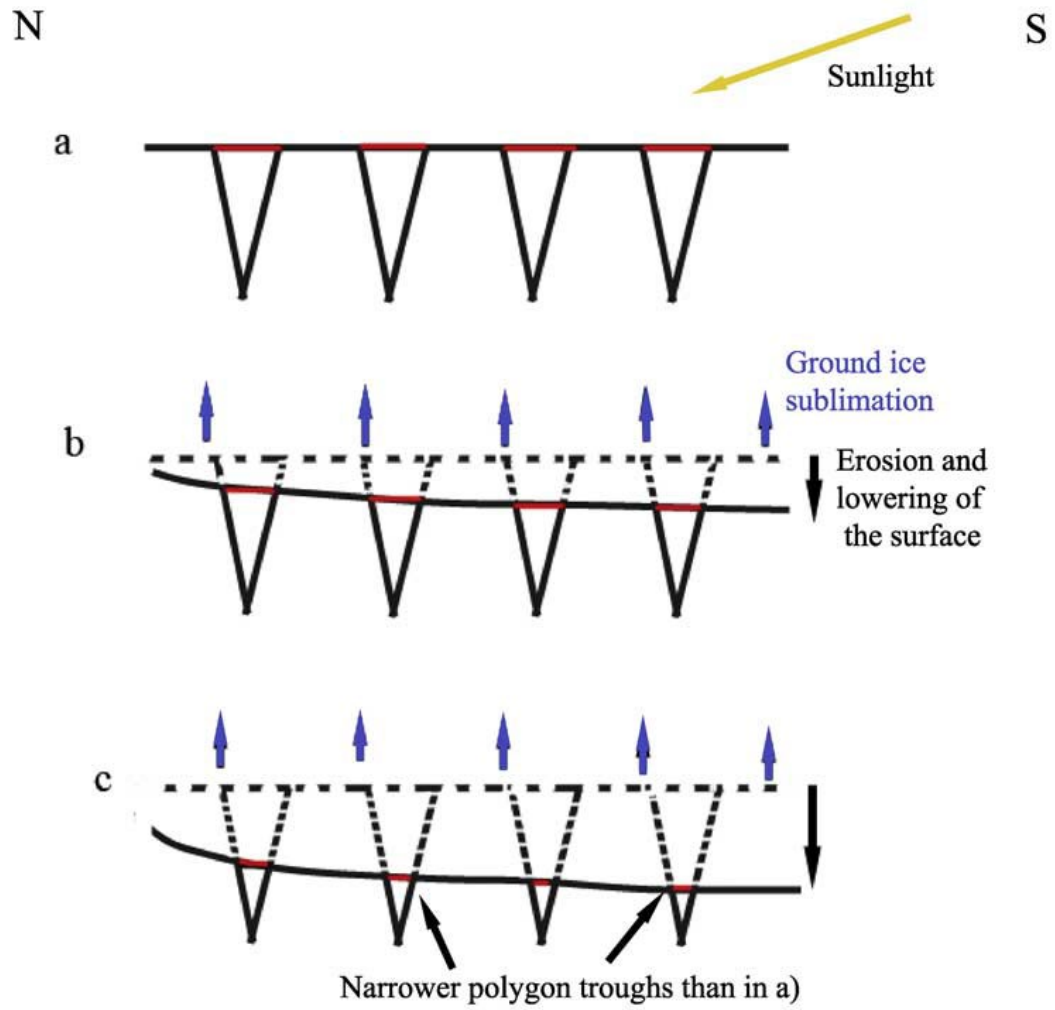

Figure 5: Downward erosion of pre-existing polygonized surface during scallop formation. Image from *Lefort* et al. (2009).

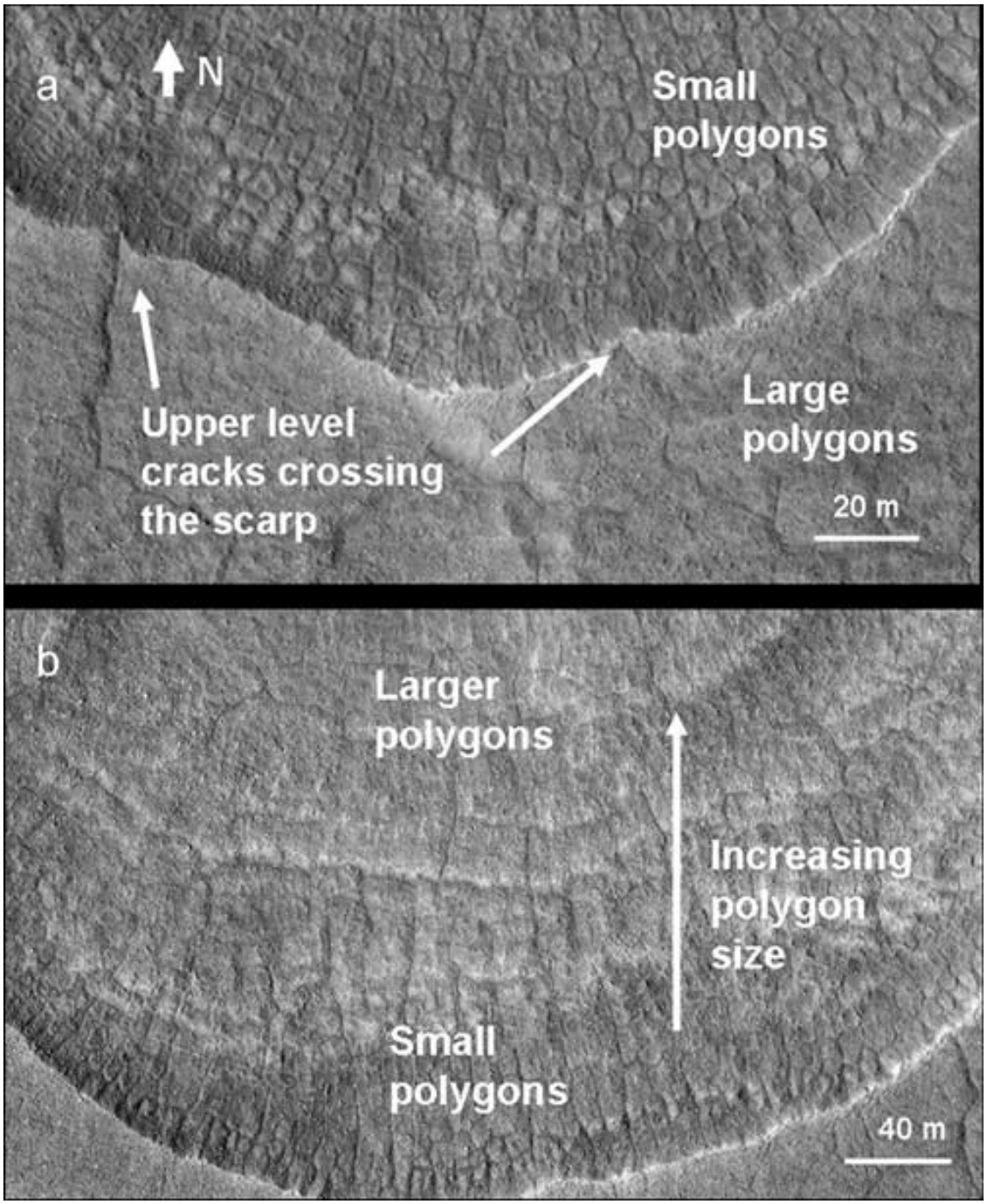

Figure 6: Demonstration of polygon size change within scallop. (HiRISE image PSP_002162_2260; 45.637°N, 93.681°E) Image from *Lefort* et al. (2009).

Scalloped depressions have been subdivided into four classes based on their observed morphologies (*Kerrigan*, 2013):

- Isolated simple scallop depressions (Figure 7a): simple circular or oval-shaped depressions that contain little to no internal complexity, most notably the ridges or "steps" that scallops often exhibit.
- Isolated complex scalloped depressions (Figure 7b): isolated simple scalloped depressions but containing internal complexity, most notable ridges or "steps" to better exemplify their gradual growth over time.
- Coalesced scalloped depressions (Figure 7c): scallops that grow so close together that they often become indistinguishable from one another.
- Crater scalloped depressions (Figure 7d): depressions formed within a crater.

Soare et al. (2015) investigated dark-toned terrain within which the scalloped depressions in Utopia Planitia are observed and noted possible layering within the walls of the depressions as well. The study hypothesized that if the dark-toned sediments were glass-rich, then they may have formed as either impact-associated ejecta or volcanoclastic sediments. *Harrison* et al. (2019) noted that the mottled tonal differences across the SDBT appear to arise from differences in dust cover based on observations in areas of concentrated dust devil tracks, revealing darker-toned material among lighter-toned areas (Figure 8).

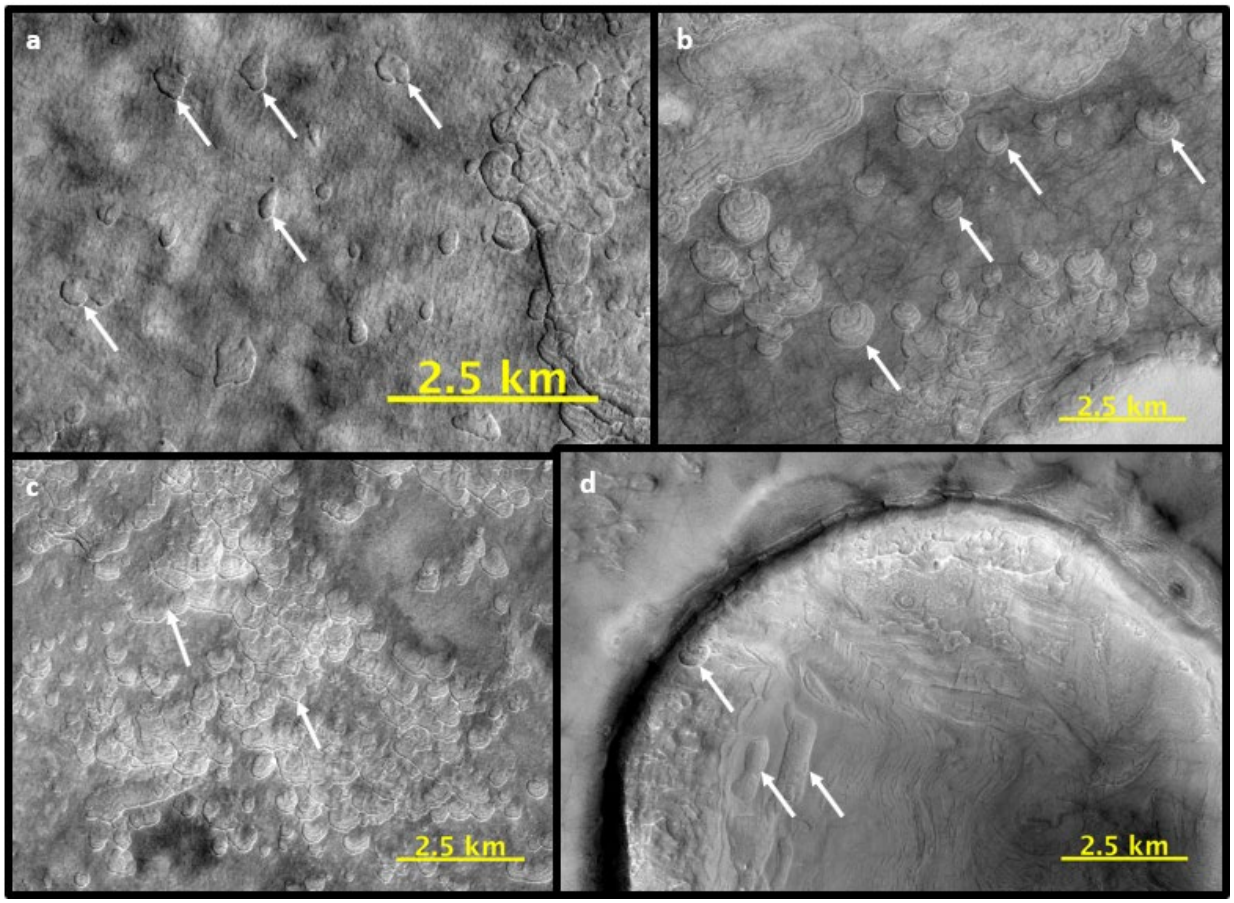

Figure 7: Types of scalloped depressions. a) Isolated simple scalloped depressions; CTX G04_019594_2267_XN_46N272W; 87.855˚E, 45.222˚N. b) Isolated complex scalloped depressions; CTX P19_008478_2246_XI_44N268W; 91.533˚E, 46.111˚N. c) Coalesced scalloped depressions; CTX P16_007476_2243_XN_44N265W; 94.533˚E, 45.642˚N. d) Crater scalloped depressions; CTX B18_016772_2318_XN_51N278W; 92.704˚E, 51.621˚N

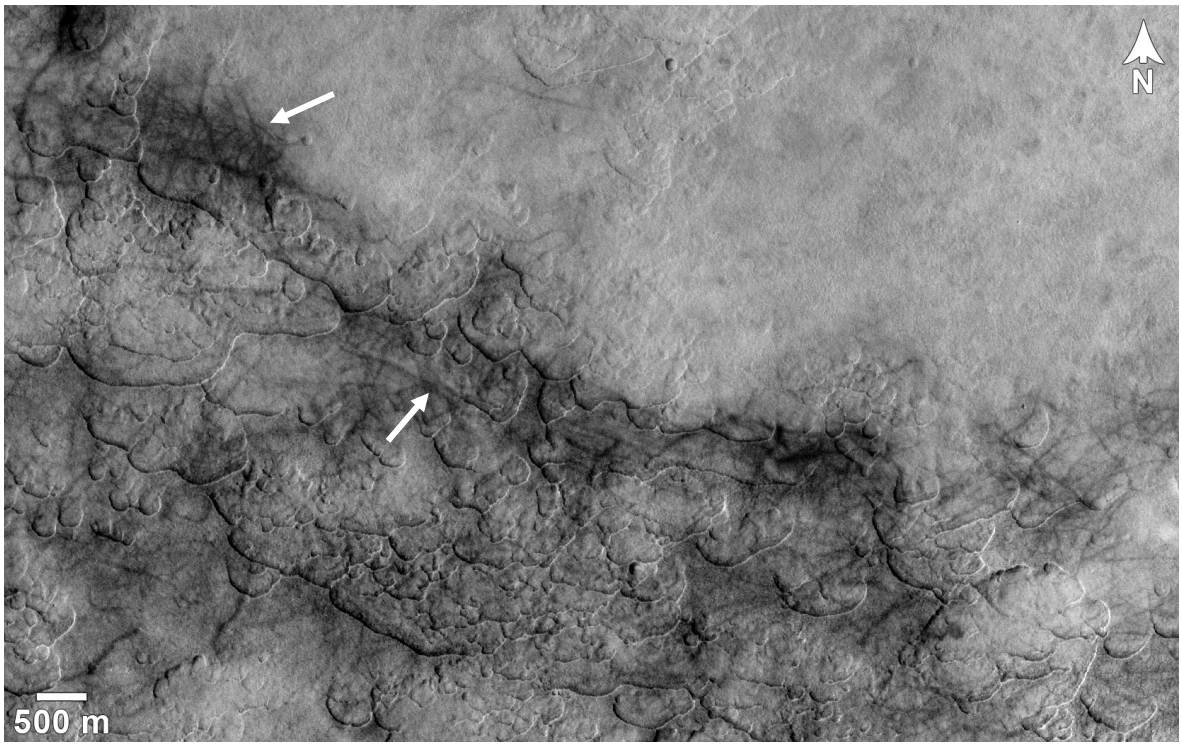

Figure 8: Example of how darker-toned terrain are concentrated in areas of dust devil tracks. Image from *Harrison* et al. (2019).

Previous Work

Kerrigan (2013) investigated the distribution and stratigraphy of scalloped depressions in Utopia Planitia in an attempt to reconstruct the past environment in which this landscape formed. The major findings of that work included the definition of a possible periglacial unit in Utopia Planitia, denoted as ABp, which was defined by its assemblage of scalloped depressions (Figure 9).

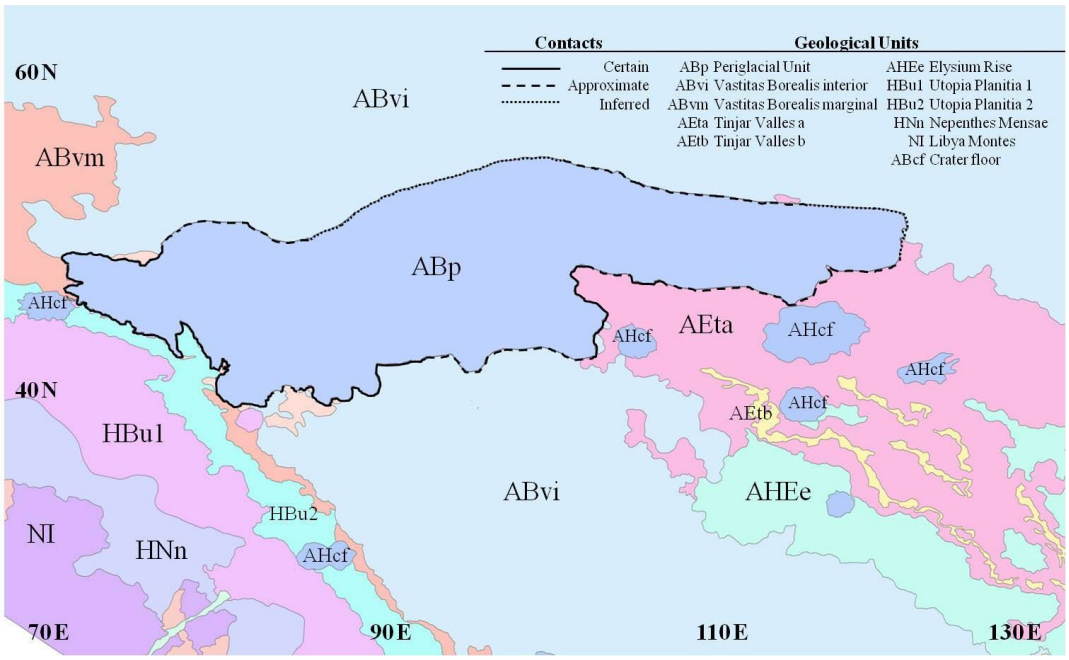

Figure 9: A revised geologic map of Utopia Planitia displaying the ABp geologic unit. Image from *Kerrigan* (2013).

This work was later complimented by *Stuurman* et al. (2016), which used Mars Reconnaissance Orbiter (MRO) SHAllow RADar (SHARAD) data to identify an expansive radar reflective region spanning approximately 375,000 km^2 (Figure 10). The primary focus of this study was southwestern Utopia Planitia where over 600 SHARAD radargrams were inspected for subsurface reflectors. Where SHARAD reflectors were discovered, it was possible to estimate the concentrations of volatiles in the subsurface where the dielectric constant could be calculated. It was determined the SHARAD reflective regions coincide with high densities of scalloped depressions and polygonal terrain. The dielectric results of *Stuurman* et al. (2016) of 2.8 ±0.8 are consistent with the material hosting scalloped depressions being comprised of porous, slightly dirty H2O ice (50-85% ice by volume) ranging in thickness from ~80-170 m.

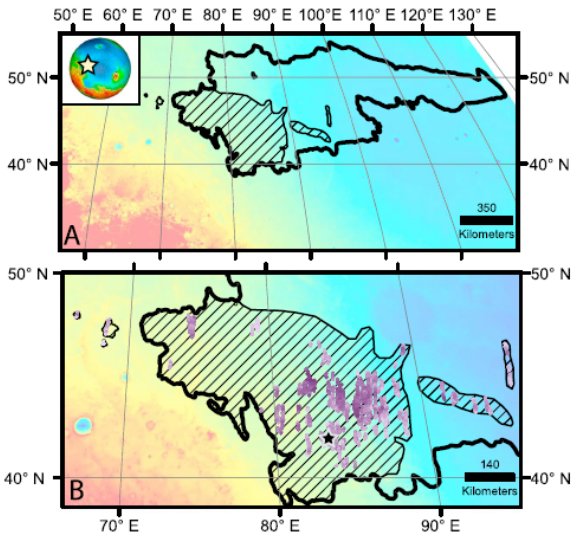

Figure 10: Geomorphological map from *Kerrigan* (2013) (Top) with SHARAD reflector region (top and bottom, striped region). Image from *Stuurman* et al. (2016).

Research Questions

Building off the work from *Kerrigan* (2013) and *Stuurman* et al. (2016), this thesis aims to answer the following questions:

1. What is the direction of growth of scalloped depressions within the mapped region?
2. How does topography affect scalloped depression growth and development?
3. What does this tell us about the geologic history of Utopia Planitia in the Late Amazonian?

We aim to accomplish this through the mapping of scalloped depressions, which will paint an accurate picture for the location, density, and direction of growth of scalloped depressions in the region. Understanding the present state of Mars' climate will ultimately help us better understand its past, as scalloped depressions allow us to not only

understand the present state of glacial retreat but will ultimately help us better understand how far this retreat has progressed.

Chapter 2: Methods and Results

Study Area

The area for this study encompasses Kerrigan's "ABp" unit stretching from approximately 35˚ to 55˚ N and 70˚ to 120˚ E, centered at approximately 98.6˚E, 47.38˚N, and spanning almost 6,500,000 km^2 (*Kerrigan*, 2013) (Figure 11).

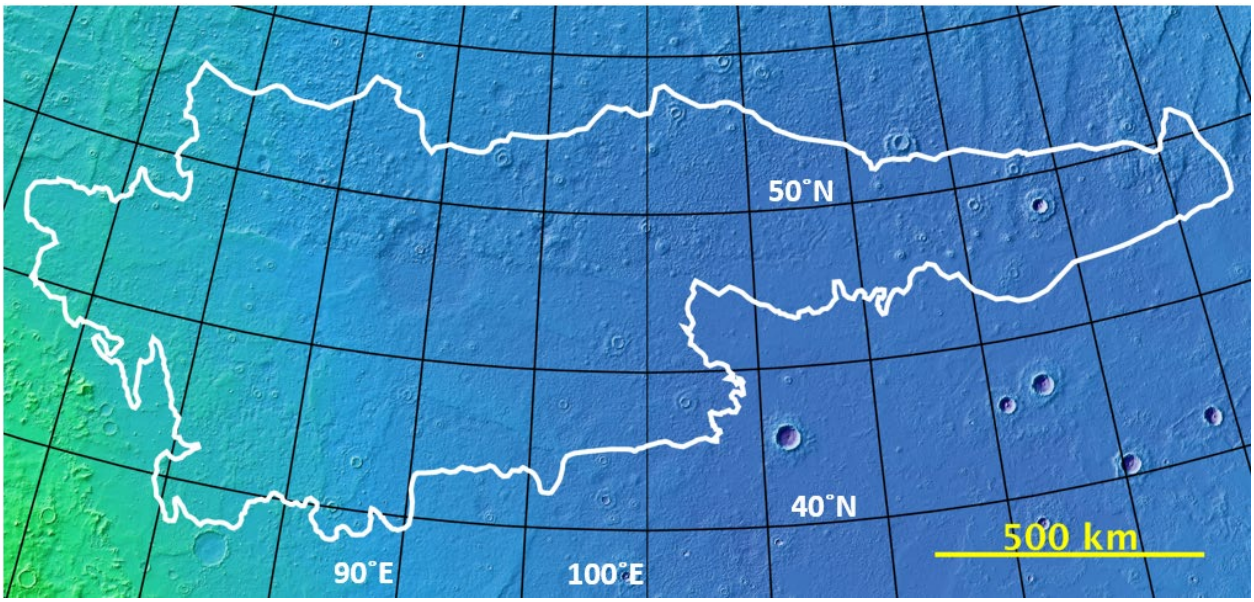

Figure 11: Study Area as previously drawn by *Kerrigan* (2013) on THEMIS Basemap

Methodology

Scalloped depressions were mapped based on clear identification of steps present within the depression itself, along with clear identification of a start and end point for each vector drawn. We inferred that the steps indicate the direction of growth and drew vectors to map the direction of scallop growth from the equator-facing slope to pole-facing scarp (Figure 12). While single scallops comprised a significant portion of the vectors drawn, we also drew vectors on coalesced scallops that still demonstrated the necessary steps within the full range of growth.

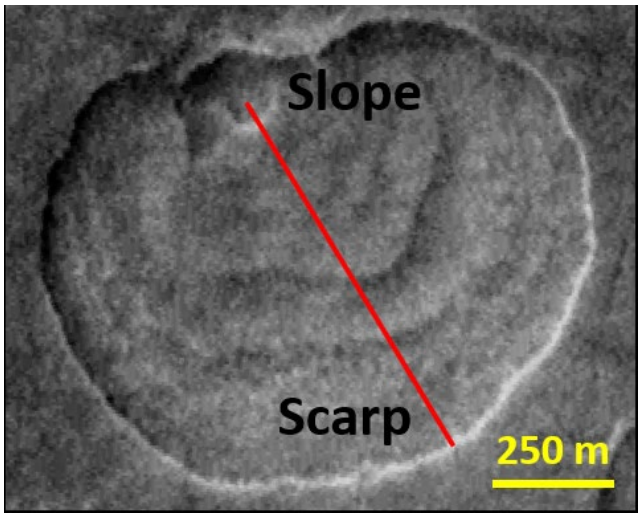

Figure 12: Example of vector drawn on a scalloped depression; CTX G18_025277_2277_XN_47N266W; 46.10˚N, 93.78˚E.

All mapping was conducted within Java Mission-planning and Analysis for Remote Sensing (JMARS) (*Christensen* et al., 2009) using Mars Reconnaissance Orbiter (MRO) Context Camera (CTX) images. Calculations to determine a correlation between elevation and latitude with scallop size were done in Microsoft Excel along with placing scallop azimuths in bins of 30˚ for sorting, and GeoRose was used to construct a scallop size diagram to determine overall directional growth of scalloped depressions.

Results

A total of 11,783 scallops were identified. 9288 scallops (78.8%) exhibit azimuths between 330˚-30˚ while the remaining 2495 (21.2%) exhibit large decreases in concentrations as the azimuth count funnels closer to 180˚ (Table 1 and Figure 13). Large decreases were observed based on the following percentages, and four bins were created, accordingly: 10-50%, 5-10%, 1-5%, and 0-1% (Table 2). Further elaboration on the results of these bins are described in the text below. With >78% of scarp azimuths ranging between 330˚-30˚, this is consistent with scallops primarily oriented in a north-

south direction (e.g., *Séjourné* et al., 2011). Scallop size and numbers appear to gradually increase until ~46˚N, then decrease at a faster rate with increasing latitude, with only sparse numbers of scallops appearing after 49˚N (Figure 14). This is consistent with previous studies showing that the number of scallops decrease with increasing latitude (*Morgenstern* et al., 2007; *Lefort* et al., 2009; *Séjourné* et al., 2011; *Harrison* et al., 2019). This latitude of 46˚N correlates with the most densely-scalloped region and lies within a region of lower crater density mapped by *Harrison* et al. (2019) (Figure 15). The scallops in this region are larger than other scallops within the study area and whose steps are extremely prominent (Figure 16a). Scallops just north of this region are smaller in appearance, and only a few scallops display prominent steps (Figure 16b). Scallops in the farthest western part of the study area are very small and their steps completely lack prominence (Figure 16c), and therefore lack the necessary criteria required for drawing vectors. An initial contact outline was drawn to identify these scallops but given their small size and lack of steps it became extremely difficult to discern them from the surrounding terrain the further east we examined.

Scallop size increased until approximately -4650 m which is the location of the most densely-scalloped region, and the size experiences a sharp decrease afterwards (Figure 17). The slight secondary rise in scallop size at approximately -4031 m occurs just outside the SHARAD reflector region but still among non-poleward scallops, while the majority of non-poleward (90˚-270˚) scallops within the SHARAD reflector region occur at ~-3700 m.

One of the objectives for this study was to determine how topography affects scalloped depression growth. It was observed that while craters within the most densely-scalloped region largely did not exhibit scallop growth atop their crater ejecta but exhibited large amounts of scallops in the surrounding region (Figure 18b), certain craters outside of the most densely-scalloped region were observed to only have scallops atop their ejecta and has sparse amounts of scallops in the surrounding region (Figures 18c & 18d). One such crater exhibited a mix between the two, where it had small amounts of scallops atop the ejecta and a larger number in the surrounding region (Figure 18e). CTX and HiRISE data sets also allowed us to identify potential scallops atop the ejecta of the largest—and possibly youngest due to lack of in-fill—crater of the study area that resides in the eastern region (Figure 19). These potential scallops were observed to exist atop the entire ejecta blanket but taper as the ejecta blanket becomes less prominent.

As noted above, scallop azimuths were placed in bins corresponding to changes in concentration, as seen in Table 2. It was observed that while scallops exhibiting azimuths from Bins 1 and 2 were mostly concentrated outside of the SHARAD reflector region (Figure 20), the majority of scallops exhibiting azimuths from Bins 3 and 4 reside either directly within or are in close vicinity of the SHARAD reflector region (Figure 21). Non-poleward facing scallops within the SHARAD reflector region are a major result of this work as they were also observed to exhibit steps that are more closely-spaced than scallops mapped in the rest of the study area (Figure 22). A brief investigation using HiRISE images also identified differences in the polygonal terrain that have been known to be a part of scallop development (*Lefort* et al., 2009) with the polygons being very

large on the upper surface and smaller within the scallop itself, then increasing in size poleward (Figure 6). However, the polygons observed within this scallop in the SHARAD reflector region exhibit the same size from within the scallop all the way to the upper surface of the pole-facing slope, except this scallop is growing from west to east (Figure 23). Further investigations using HiRISE and HiRISE DTMs is recommended to better understand the growth and development of these particular scallops.

While scallops were the focus of this study, we observed a few landforms of possible periglacial origin that stood out amongst the landscape. These landforms have the initial appearance of scalloped depressions, but do not exhibit the steps that were the primary criteria for mapping scallops (Figure 24). These features are unique because they reside in a region entirely devoid of scallops.

Azimuth (deg)	Count	Percentage
0-30	3777	32.05%
30-60	635	5.39%
60-90	146	1.24%
90-120	36	0.31%
120-150	15	0.13%
150-180	5	0.04%
180-210	24	0.20%
210-240	78	0.66%
240-270	154	1.31%
270-300	258	2.19%
300-330	1144	9.71%
330-360	5511	46.77%
Grand Total	**11783**	**100.00%**

Table 1: Scallop azimuth totals

Bin	Azimuth (deg)	Count	Percentage
1	330-30	9288	78.80%
2	30-60, 300-330	1779	15.10%
3	60-90, 240-300	558	4.74%
4	90-240	134	1.34%

Table 2: Re-sorted bins based on percentage changes

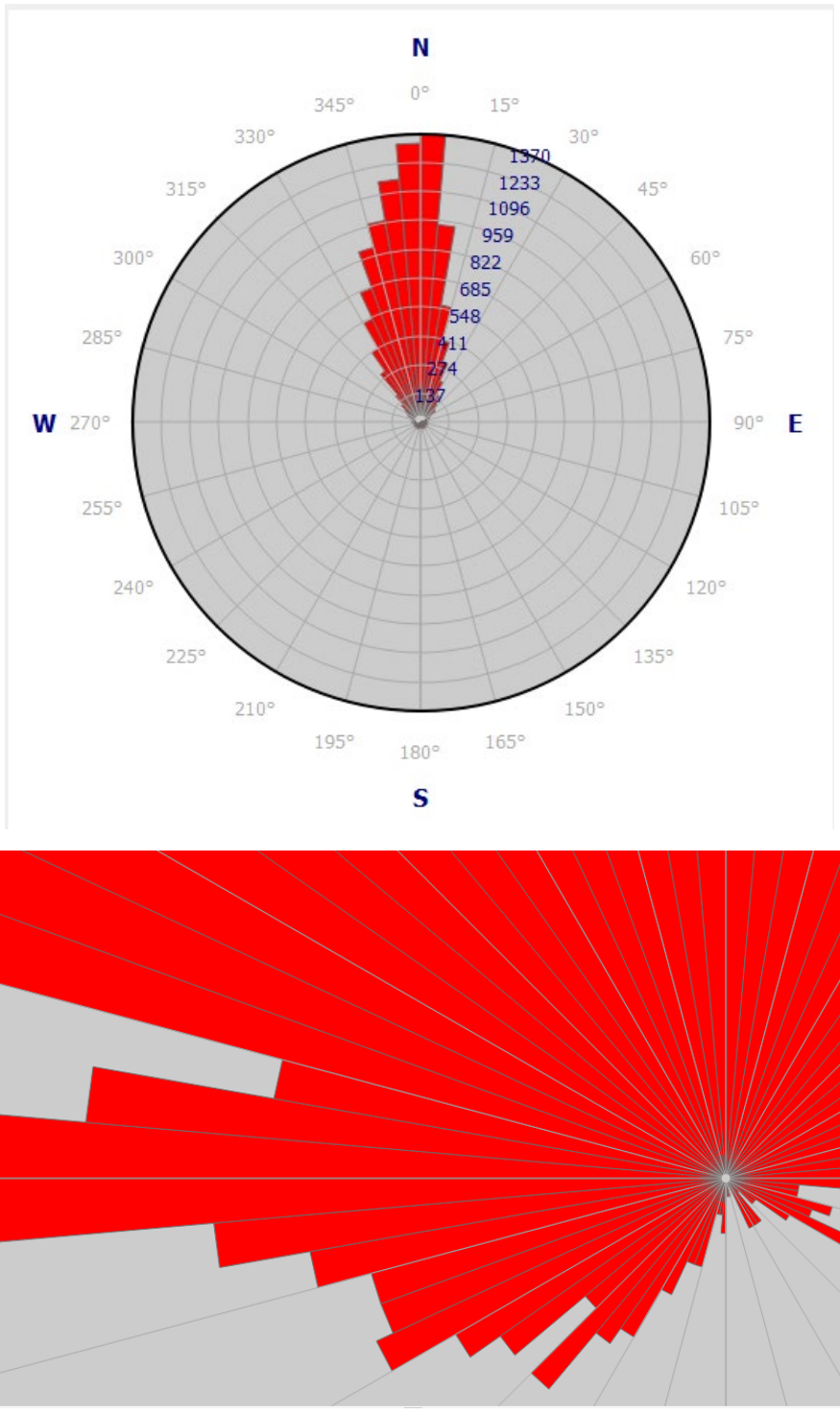

Figure 13: Of the 11,783 scallops that were mapped, 9288 scallops (78.82%) exhibit azimuths between 330˚ and 30˚ (top). 311 scallops exhibited azimuths between 90˚ and 270˚, which were considered non-poleward-facing azimuths (bottom).

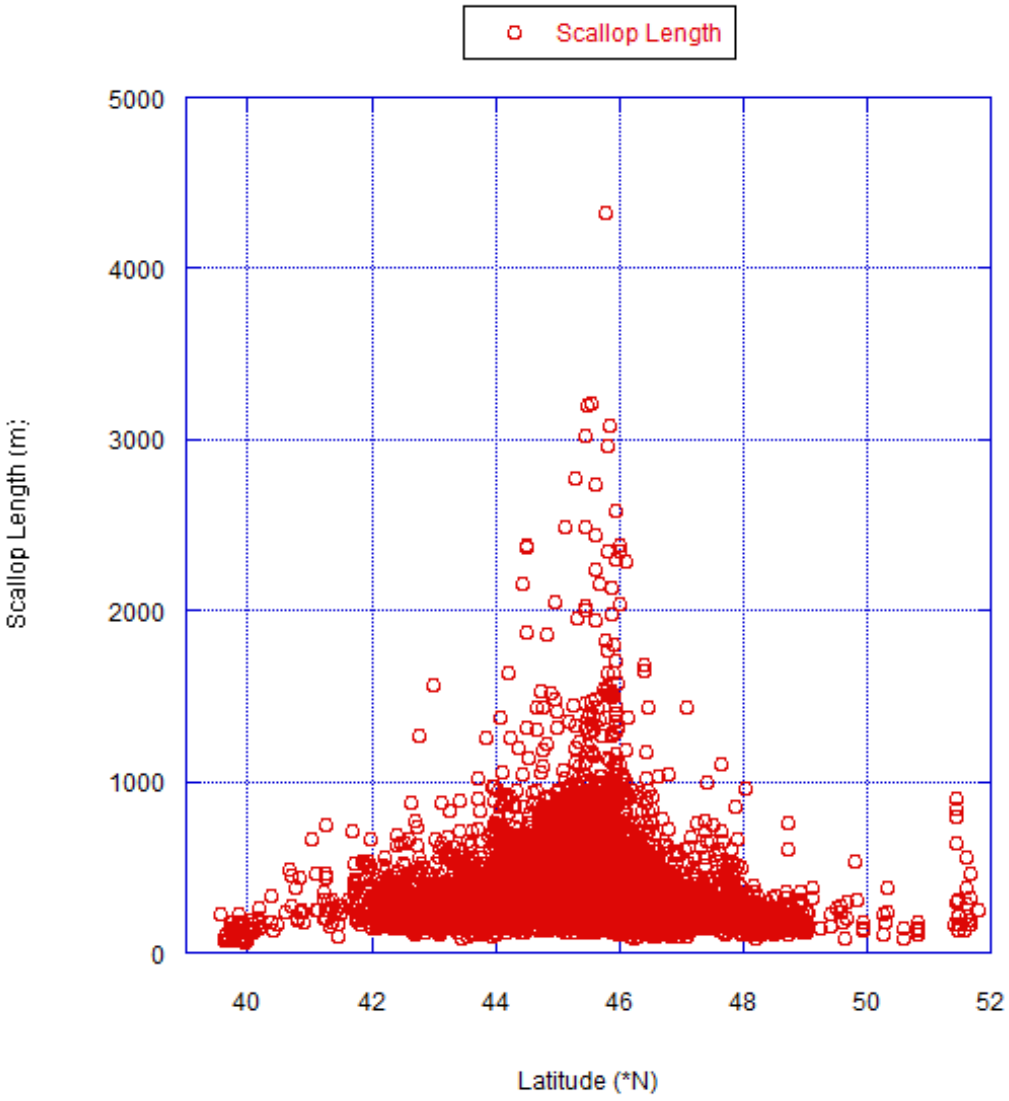

Figure 14: Graph showing relationship between latitude and scallop size

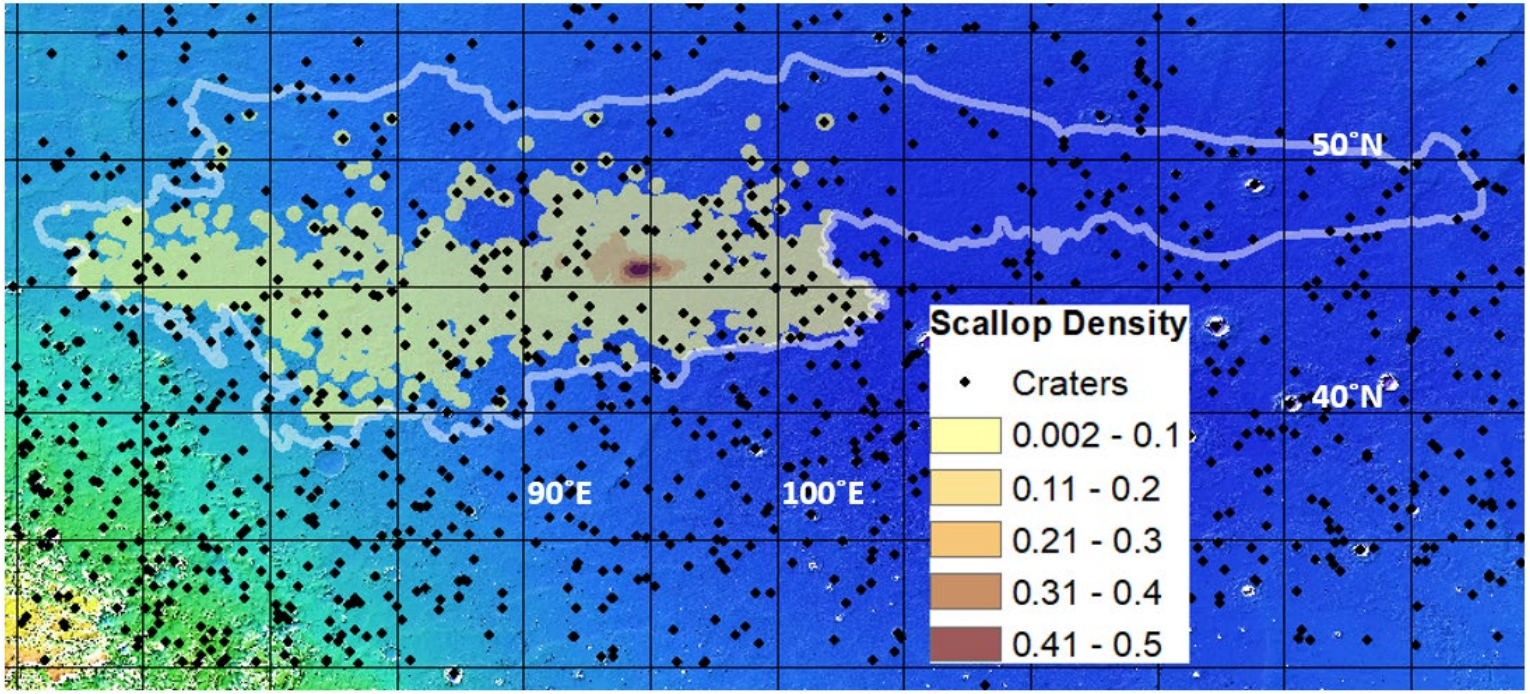

Figure 15: Density plot of scallops within *Kerrigan* (2013) study area (white outline) with black dots denoting craters from *Harrison* et al. (2019) on MOLA Basemap

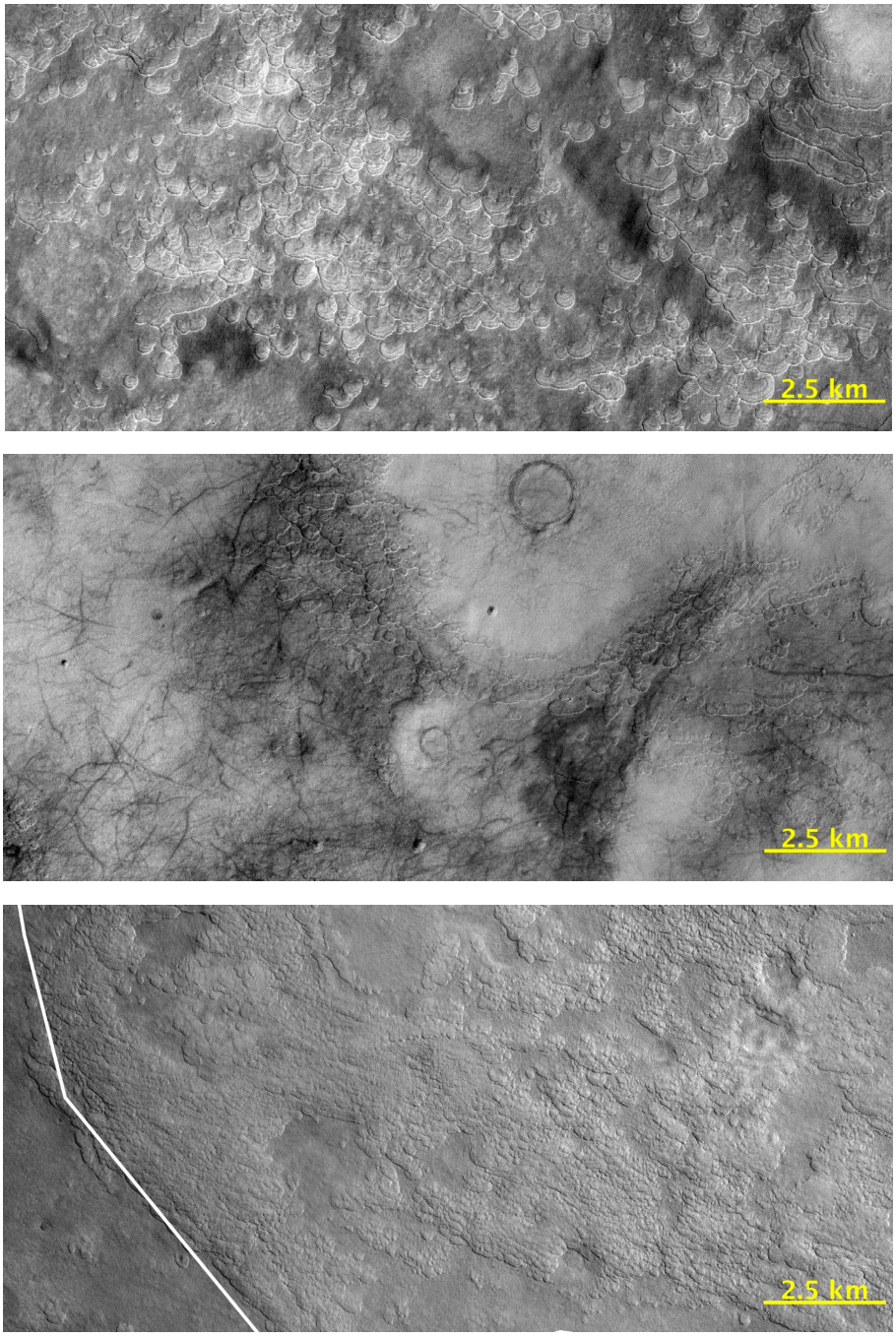

Figure 16: Examples of different sized scallops throughout the study area. See text for description. a) CTX P16_007476_2243_XN_44N265W and G20_026055_2240_XN_44N264W; 45.635˚N, 94.589˚E; b) CTX G01_018763_2302_XI_50N265W, G01_018618_2301_XI_50N265W, and F04_037171_2317_XN_51N265W; 49.422˚N, 94.451˚E; c) CTX B18_016575_2255_XN_45N288W; 46.809˚N, 71.291˚E

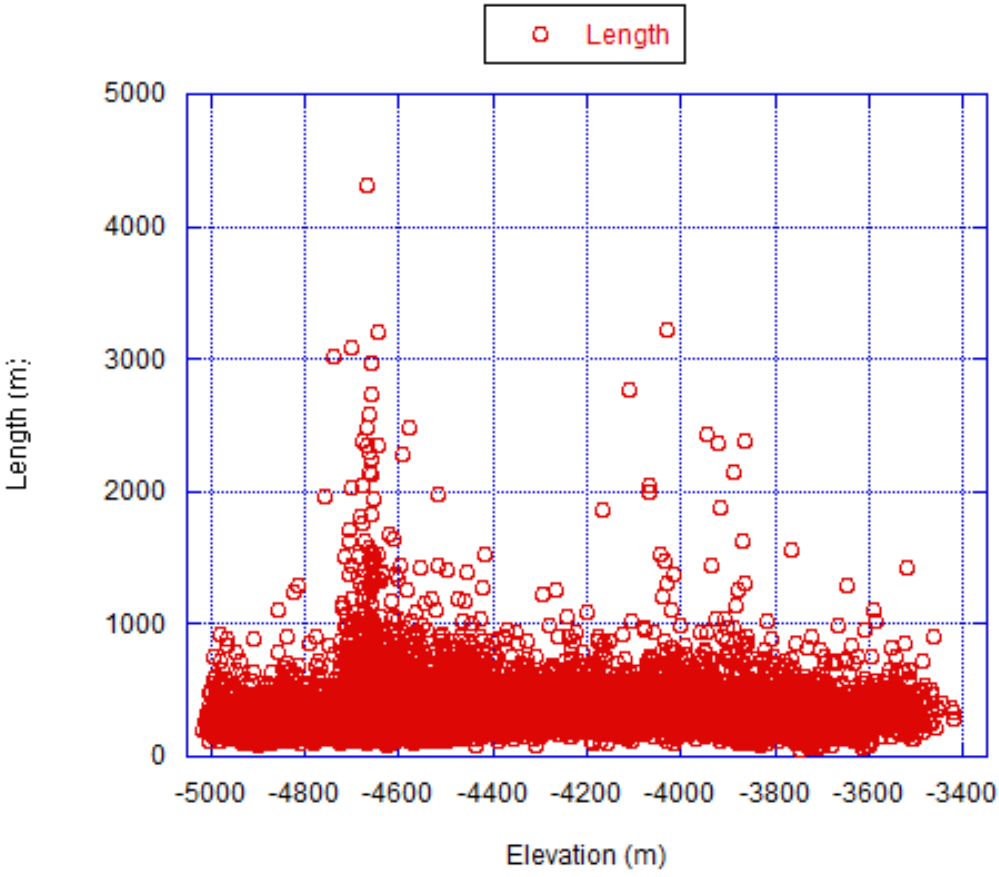

Figure 17: Graph showing relationship between elevation and scallop size

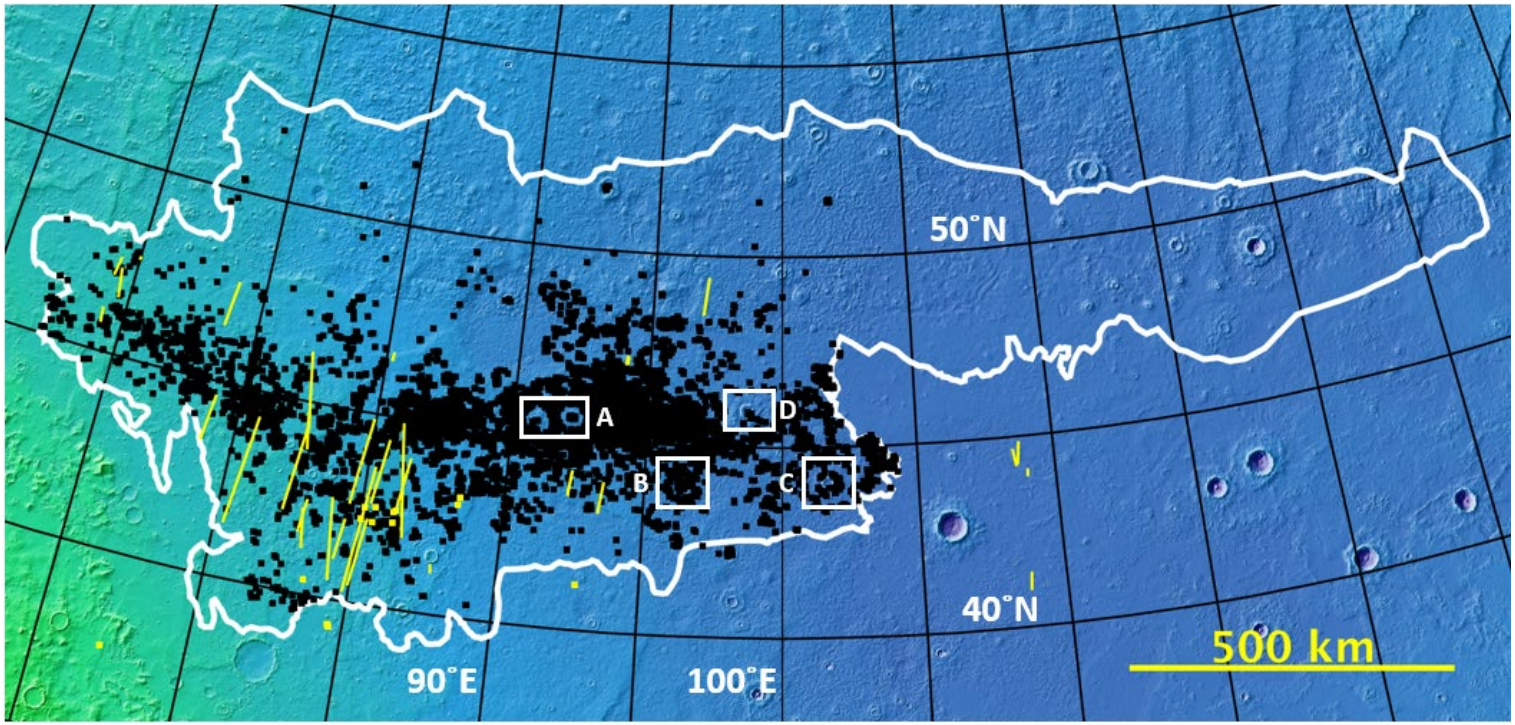

Figure 18a: Locations of crater ejecta (a, b, c, and d) with scallops as points (black) within the study area with SHARAD reflectors (yellow).

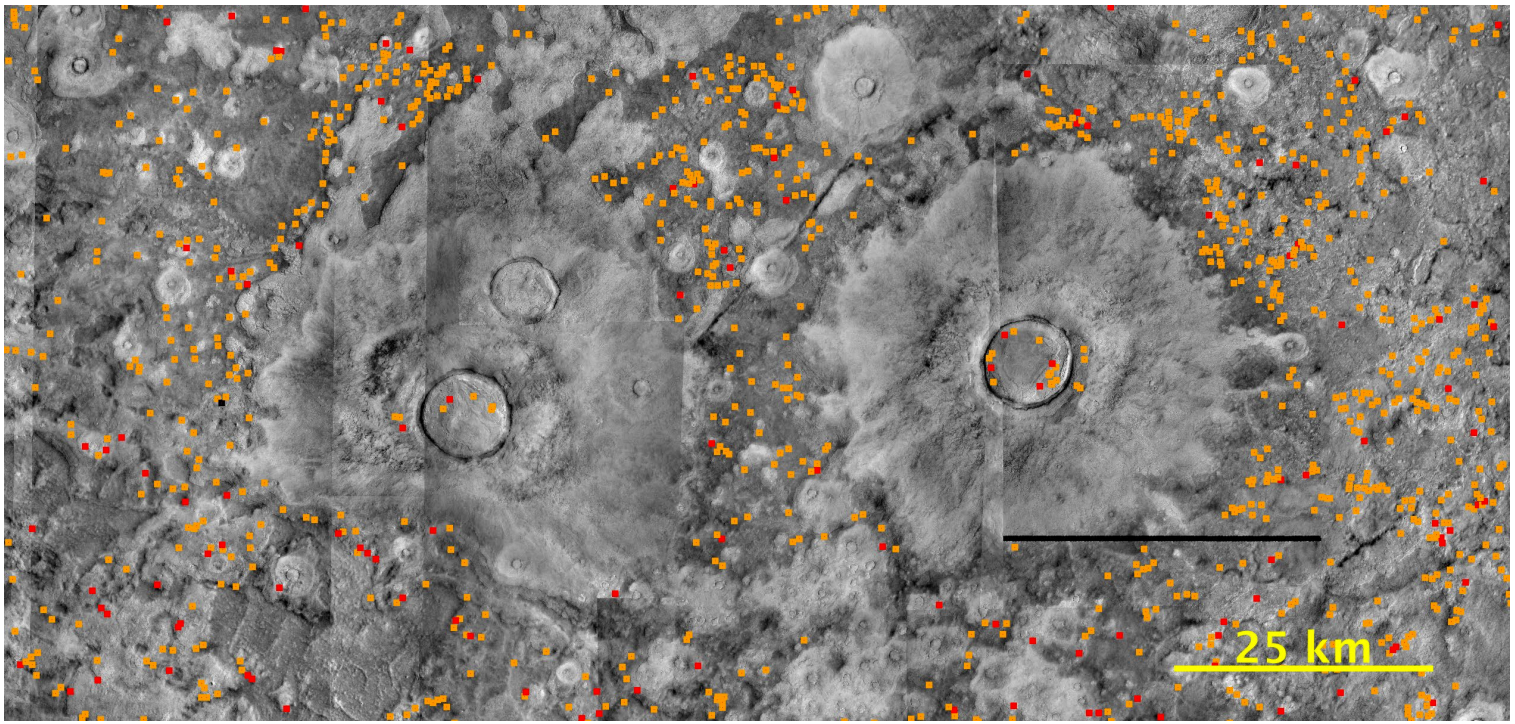

Figure 18b: Examples of craters within the most densely-scalloped region that largely did not exhibit scallop growth atop their ejecta but exhibited large amounts of scallops in the surrounding area while demonstrating azimuths of 330˚-30˚ (Orange), 90˚-270˚ (Black), and all others (Red); CTX images; 91.55˚E, 45.51˚N

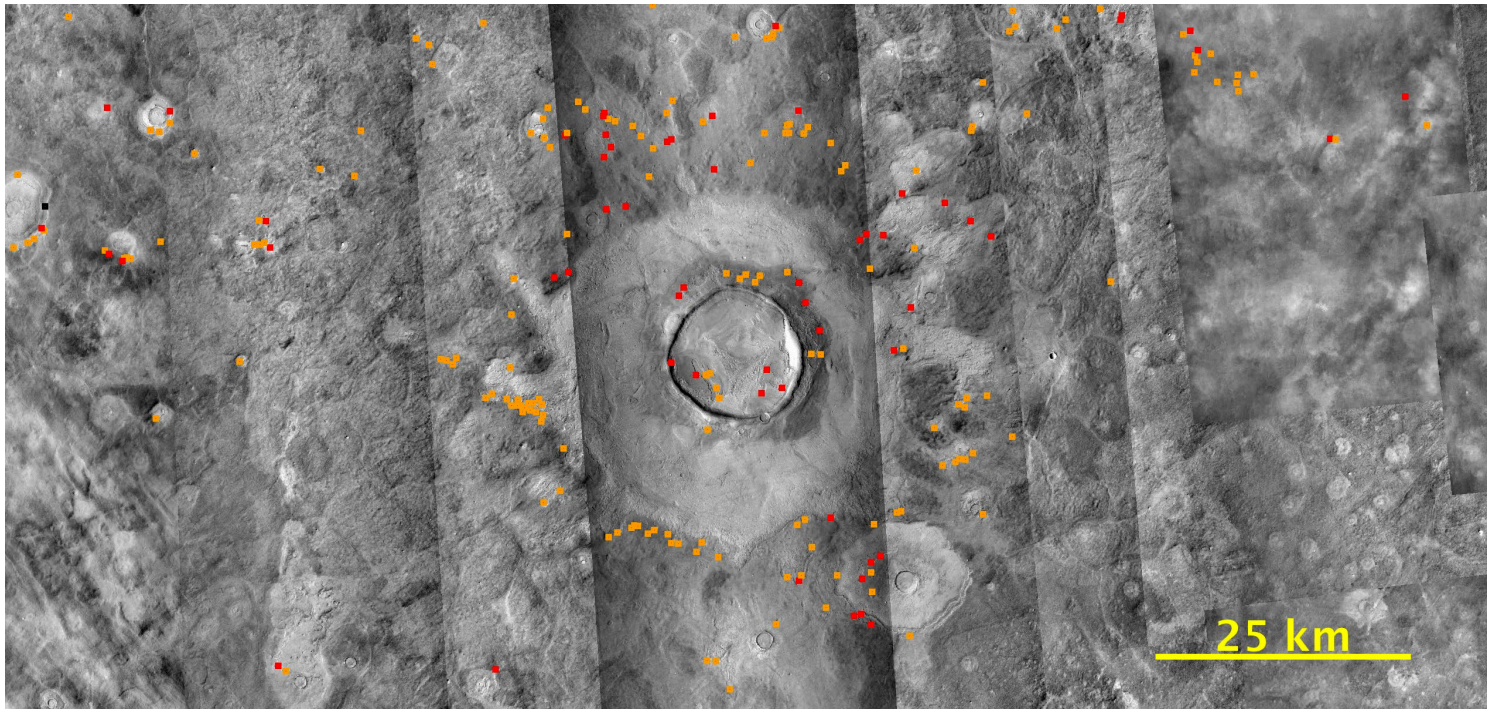

Figure 18c: Example of a crater outside of the most densely-scalloped region observed to only have scallops atop their ejecta and sparse amounts of scallops in the surrounding area while demonstrating azimuths of 330˚-30˚ (Orange), 90˚-270˚ (Black), and all others (Red); CTX images; 96.387˚E, 43.927˚N

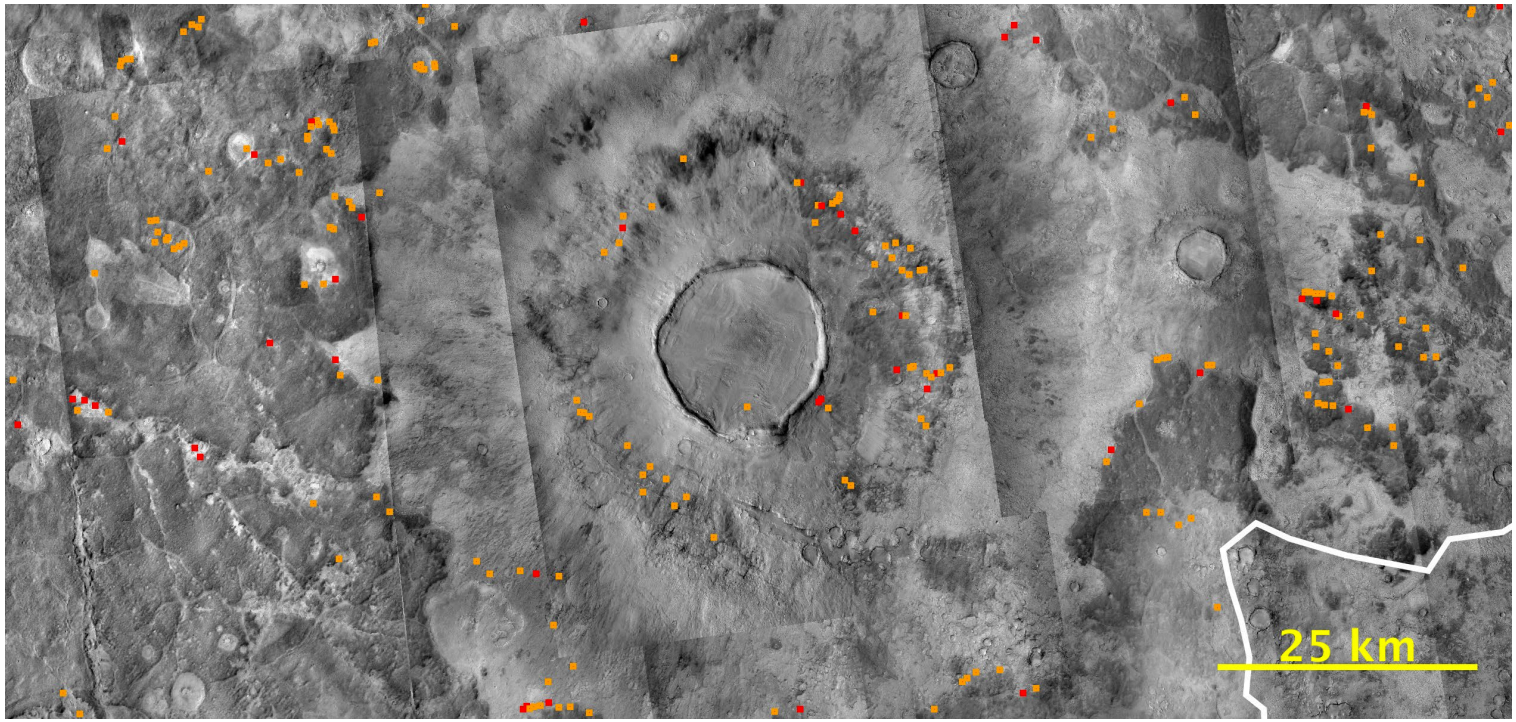

Figure 18d: Example of a crater outside of the most densely-scalloped region observed to only have scallops atop their ejecta and sparse amounts of scallops in the surrounding area while demonstrating azimuths of 330˚-30˚ (Orange), 90˚-270˚ (Black), and all others (Red); CTX images; 101.746˚E, 44.011˚N

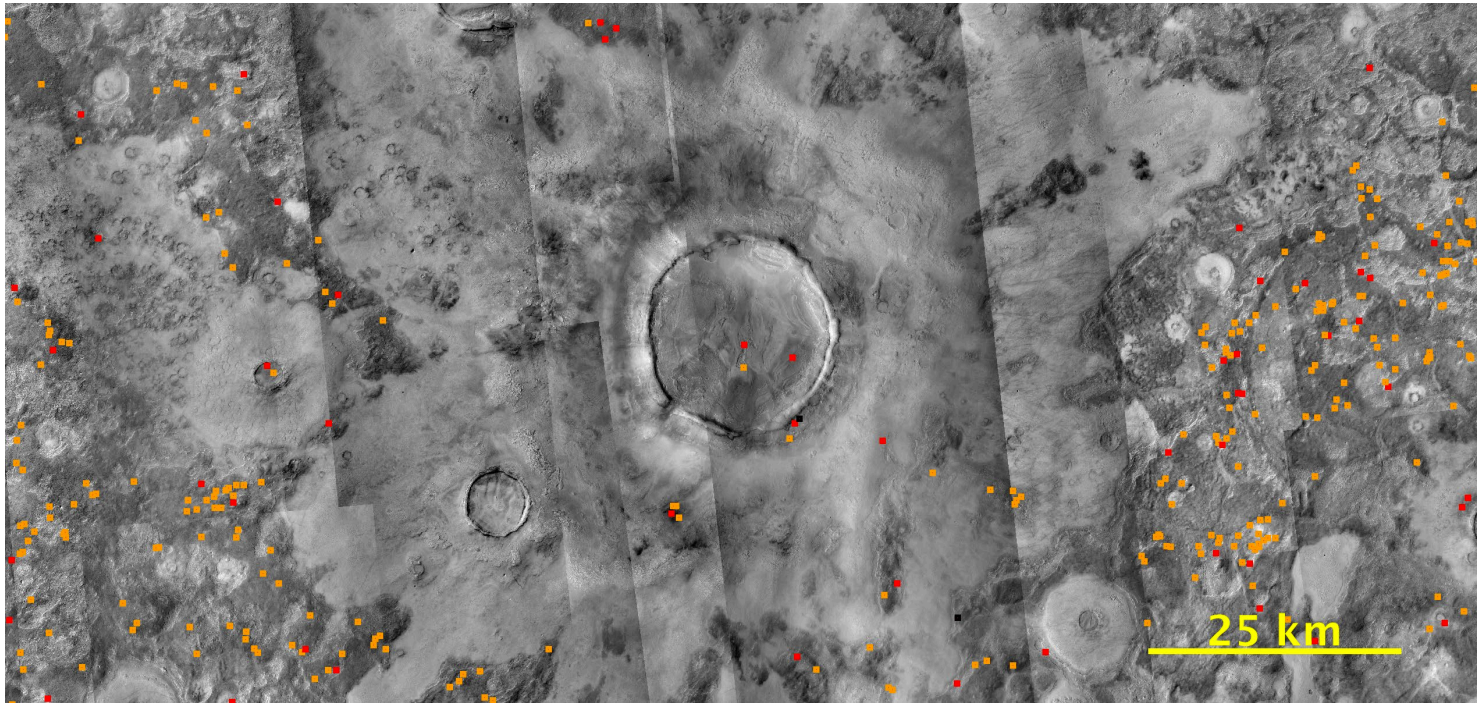

Figure 18e: Example of a crater exhibiting small amounts of scallops atop their ejecta and a larger number in the surrounding region while demonstrating azimuths of 330˚-30˚ (Orange), 90˚-270˚ (Black), and all others (Red); CTX images; 98.728˚E, 45.891˚N

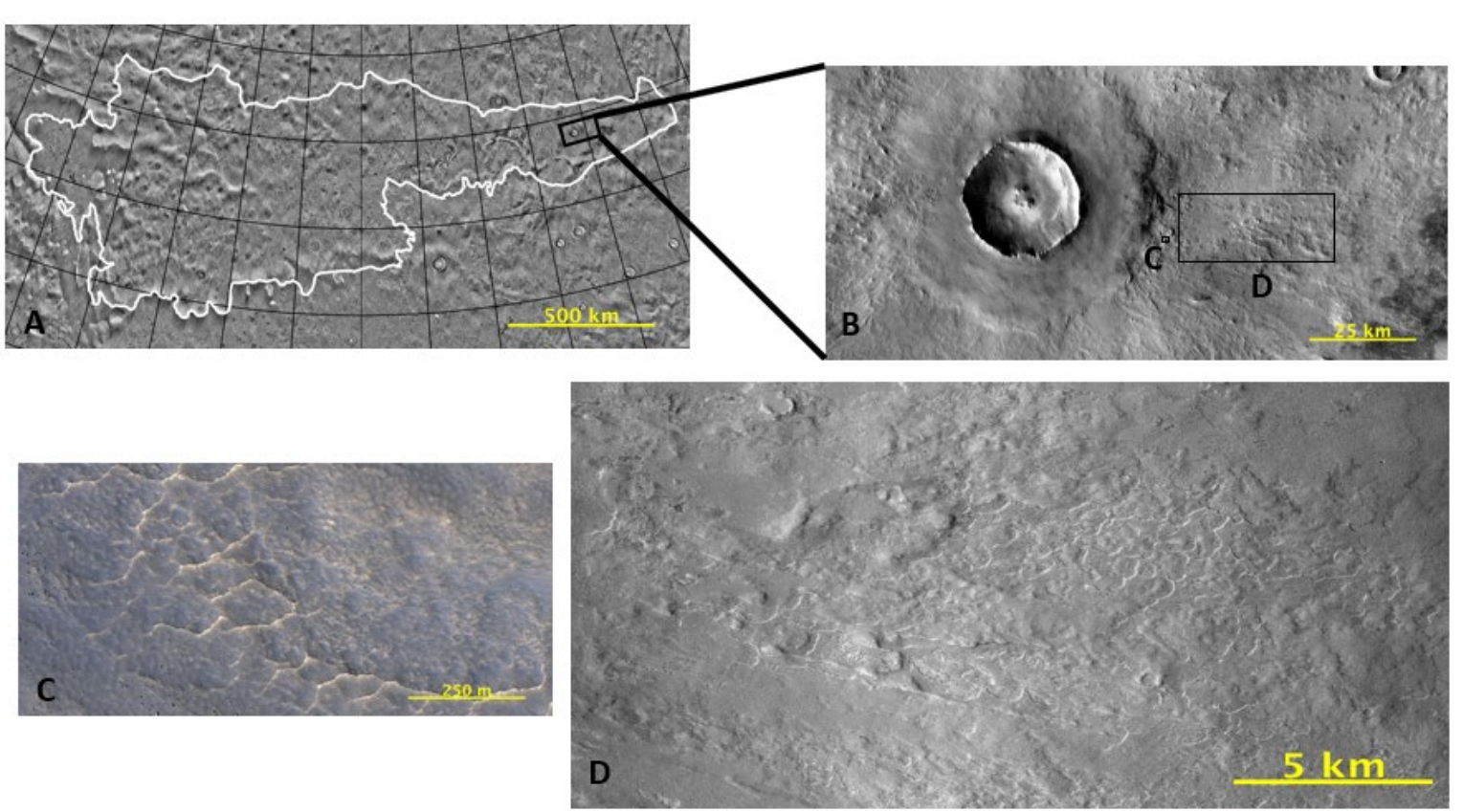

Figure 19: Potential scallops residing atop crater ejecta in the eastern region of the study area. a & b) THEMIS Basemap; c) HiRISE ESP_045544_2290_COLOR; 119.717˚E 48.819˚N. d) CTX G22_0266876_2284_XN_48N239W; 120.279˚E 48.867˚N

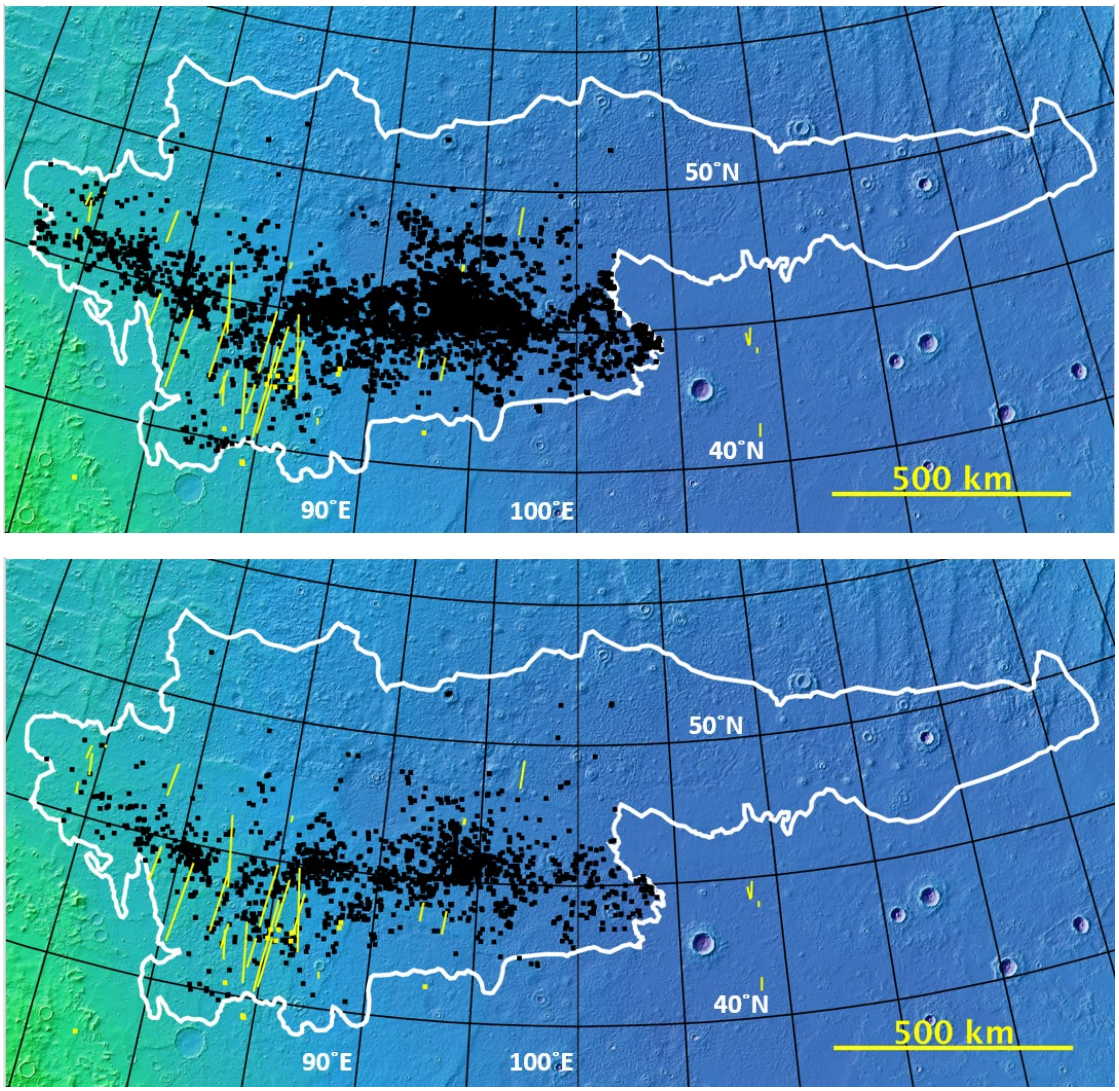

Figure 20: Scallop azimuths of Bin 1 (top) and Bin 2 (bottom) demonstrate higher concentrations outside of the SHARAD reflector region (yellow lines).

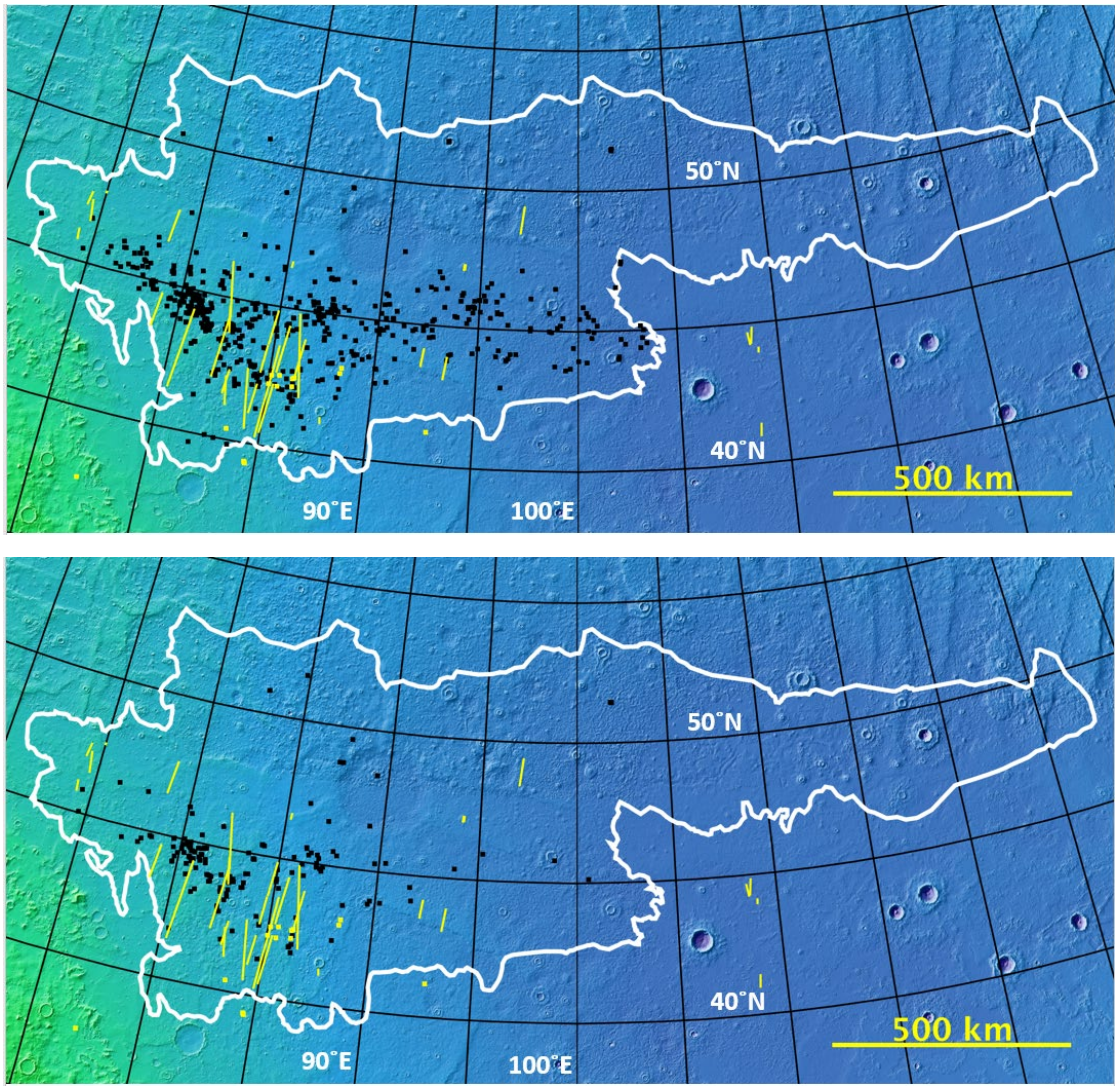

Figure 21: Scallop azimuths from Bin 3 (top) and Bin 4 (bottom) resided within or close vicinity of the SHARAD reflector region (yellow lines).

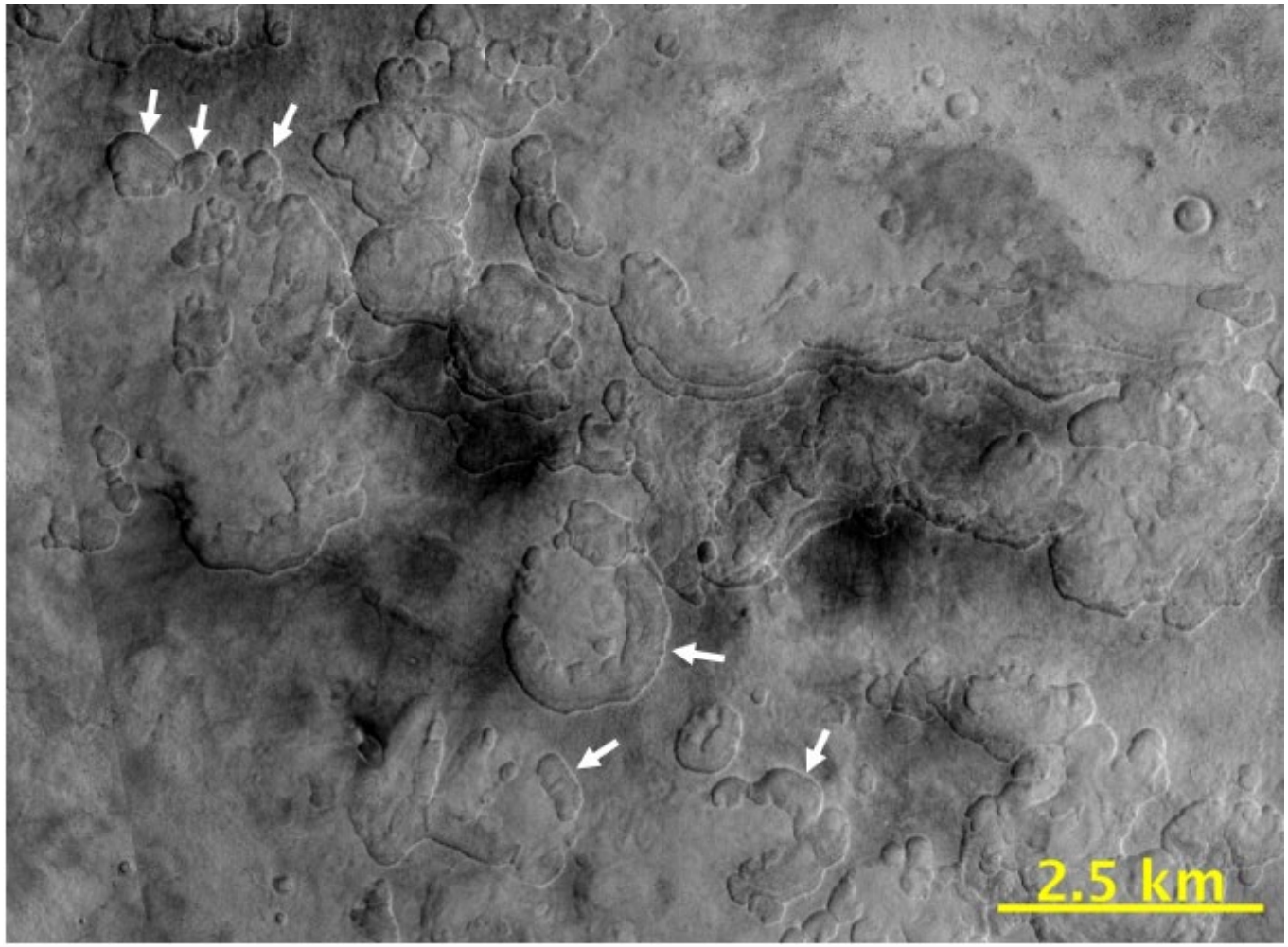

Figure 22: Scallops within the SHARAD reflector region exhibiting more closely-spaced steps than typically observed (white arrows), CTX D03_028271_2247_XI_44N279W and G23_027150_2238_XN_43N278W; 80.59˚E, 44.72˚N

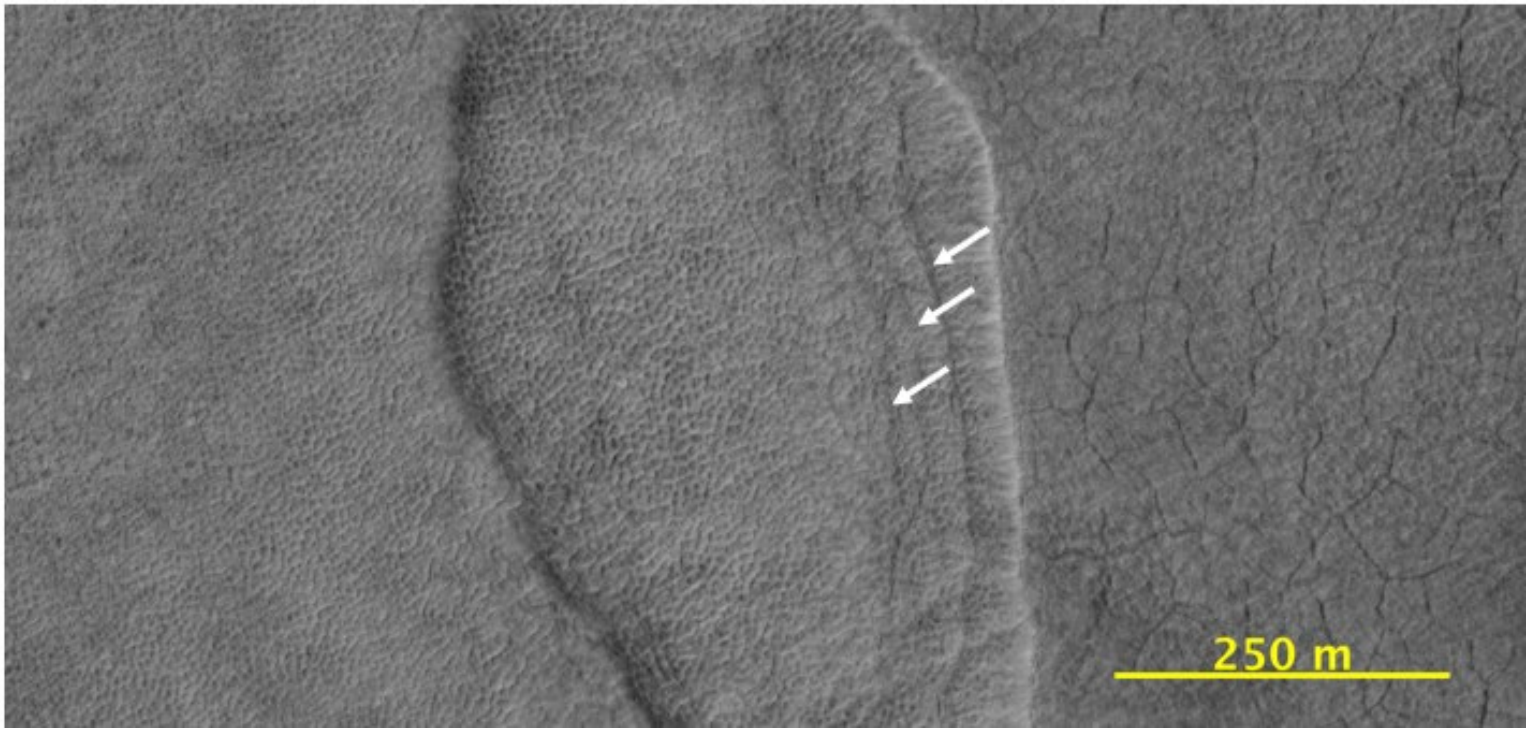

Figure 23: Scallop within the SHARAD reflector region with more closely-spaced steps and polygonal terrain that remains uniform throughout parts of the upper surface and scallop; HiRISE B17_016390_2231_XN_43N278W; 81.625˚E, 43.881˚N

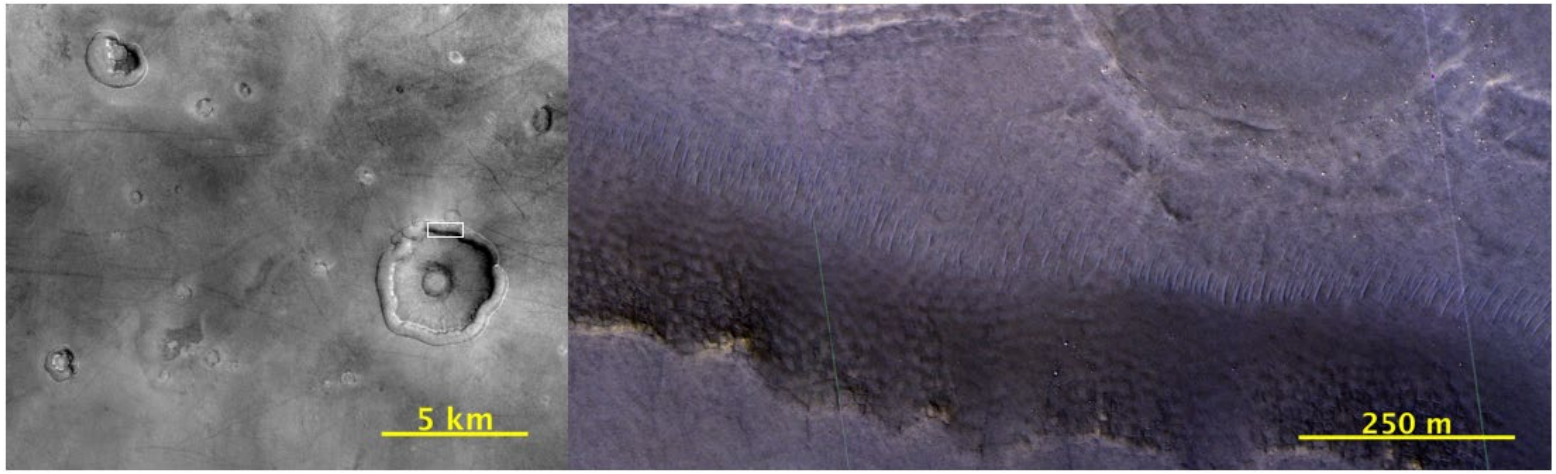

Figure 24: Possible periglacial landforms that have the initial appearance of scallops but lack steps and also devoid of scallops in immediate vicinity. Aeolian bedforms within moat (inset); CTX D17_033809_2315_XN_51N275W; HiRISE ESP_033242_2315_COLOR; 51.112˚N, 84.430˚E

Chapter 3: Interpretations and Discussion

The scalloped-depression-bearing terrain (SDBT) (*Harrison* et al., 2019) extends from ~38-54˚N and 70-128˚E to the margins of the possible periglacial unit "ABp" mapped by *Kerrigan* (2013), which is defined by the presence of scallops. An outcome of our more complete identification of scalloped depressions within Utopia Planitia is the potential to refine the extent of scallops as mapped by *Kerrigan* (2013), specifically east of 102˚ E due to the negligible number of scalloped depressions found here (Figure 25). While the *Kerrigan* (2013) study only had ~75% CTX coverage of the total study area, our study has close to 100% CTX coverage. *Kerrigan* (2013) stated, "In the east of the area of 102˚ E, the terrain in which the scalloped depressions occur becomes intermittent with terrain that is generally smoother and has a higher albedo." While we identified potential scallops within a young crater in the eastern region (Figure 19), our criteria for

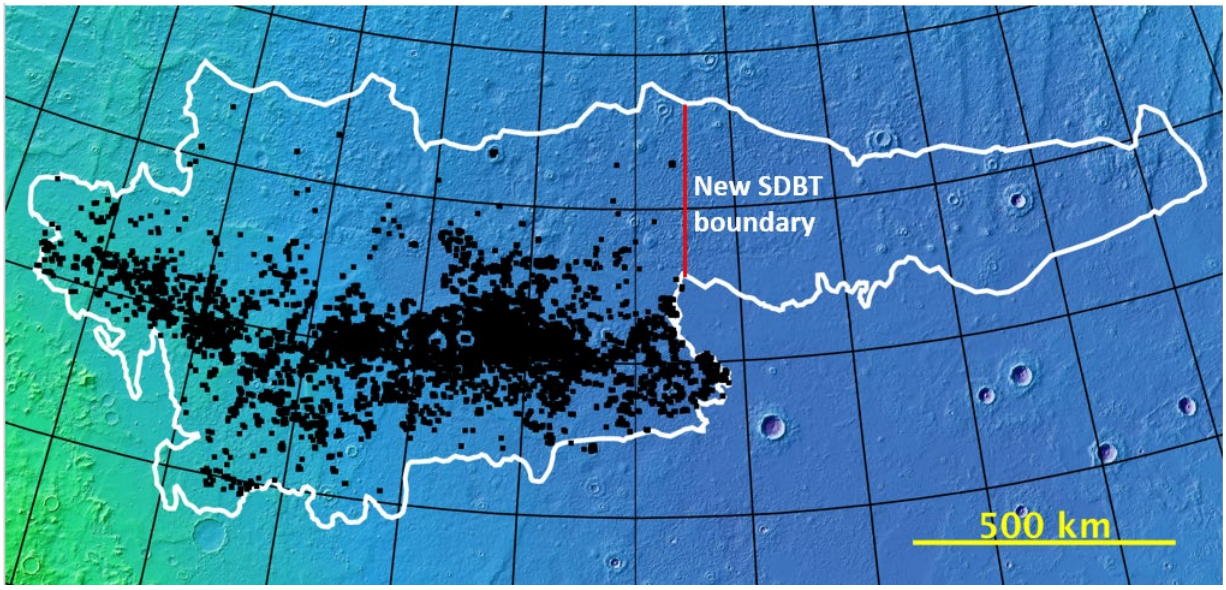

Figure 25: Refined SDBT map from *Kerrigan* (2013) with white line indicating refined extent of SDBT terrain. Lat/long has 5˚x5˚ spacing.

identifying scalloped depressions, specifically using steps as the primary identifier, subsequently removes the entire eastern region of Kerrigan's mapped region.

The story of relating topography to scalloped depression development can best be told by the most densely-scalloped region, which occurs within a lower spatial density of craters mapped by *Harrison* et al. (2019). *Séjourné* et al. (2011) and *Harrison* et al. (2019) both discuss how aeolian activity plays a role in removing surface lag deposits which exposes near-surface ice to sublimation. The ice then sublimates, creating a lag to protect once-deeper ice. Aeolian processes remove this lag, exposing more ice to unstable surface

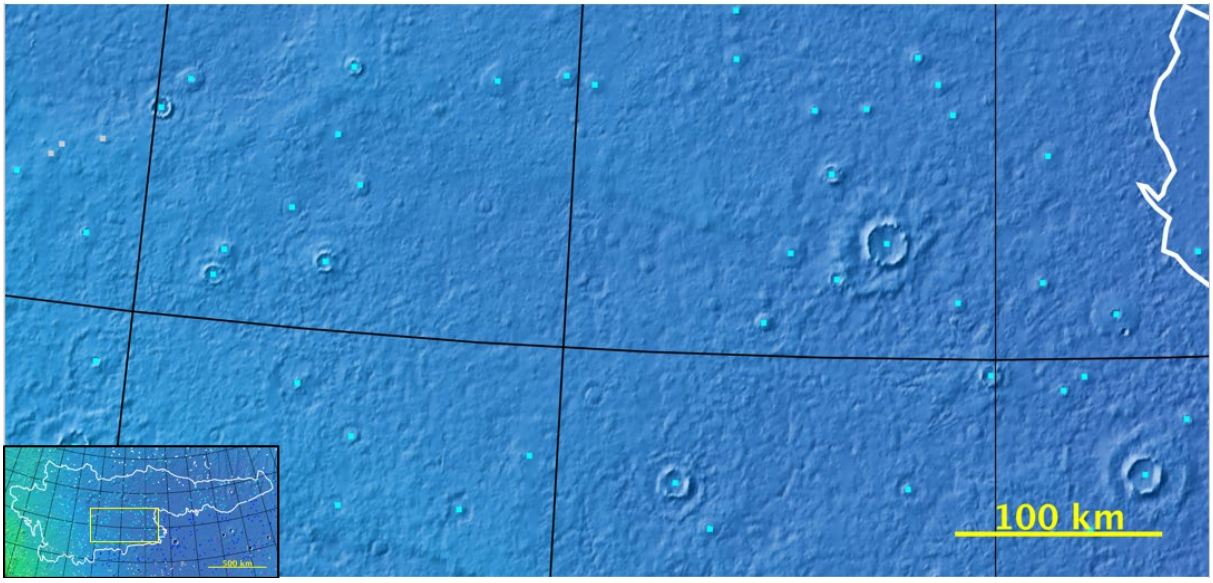

Figure 26: Most-densely scalloped region resides within an area with a low spatial density of craters mapped by *Harrison* et al. (2019).

conditions, resulting in more sublimation, and the cycle repeats. This topographic-low basin with a low spatial density of craters (Figure 26) could allow for greater aeolian processes to occur along with greater temperatures due to a thicker atmosphere. This creates a greater feedback cycle involving larger amounts of dust removal, leading to greater ice sublimation, thus larger scallops.

Séjourné et al. (2011) developed a six-stage conceptual model proposing equatorward expansion of scalloped depressions during high-obliquity periods on Mars (~45˚). This model begins with initial shallow depressions. Increased solar radiance along the pole-facing slopes (areas that are normally shadowed except at high obliquity) leads to rapid ice sublimation, collapse, and scarp retreat. Wind may then remove sublimation lag (*Harrison* et al., 2019), deepening the scalloped depressions we see today. Maximum solar radiance along the equator-facing slopes is experienced throughout the entire range of obliquities, preventing large scale ice deposition possibly resulting in a much gentler slope.

We illustrate this conceptual model to the most densely-scalloped region of our study area (45˚N) during periods of present obliquity (25˚) and high obliquity (45˚) (Figure 27). During periods of high obliquity and in northern summer, the pole-facing scarps receive maximum solar insolation (solar incidence angle of 0˚ on a flat slope) relative to today (solar incidence angle of 20˚). During periods of present obliquity, the pole-facing scarps receive less solar insolation resulting in an environment more favorable to volatile (ice) accumulation. Along with *Séjourné* et al. (2011), we propose this accumulated ice undergoes rapid removal during periods of high obliquity when the host soils collapse,

resulting in the steep-sided scarps we see today. All scallops begin with an initial depression (Step 1). Over time, aeolian processes may slowly remove the upper surface exposing the ground ice beneath along with gradual build-up of ground ice along the pole-facing scarp due to the lack of solar insolation (Step 2). Solar insolation along the equator-facing slope causes the now-exposed ground ice to sublimate with ground ice along the pole-facing scarp continuing to build up (Step 3). The now-sublimated ground ice leaves behind remnants of the ice/dust layer beneath after sublimation, resulting in gentler equator-facing slope (Step 4). Aeolian processes return and gradually remove the upper surface and the process repeats (Step 5).

Upon returning to periods of high obliquity (45˚), the entire depression now experiences full solar insolation due to the solar incidence angle now being at 0˚ (Step 6). Aeolian processes once again gradually remove the upper surface exposing the ground ice beneath (Step 7). The ground ice along the equator-facing slope once again sublimates, but with the larger amount of ground ice along the pole-facing scarp now receiving a larger amount of solar insolation (Step 8). The larger amount of ground ice along the pole-facing scarp sublimates causing a collapse in the upper surface and the first "step" of a scallop is now created (Step 9). Aeolian processes once again gradually remove the upper surface where further sublimation possibly occurs, although at much smaller rates (Step 10).

Lefort et al. (2009) discuss how each step within a scallop could correspond to a different period of high obliquity, and that the presence of two or three interior ridges suggest that the formation of larger scallops has occurred over several obliquity cycles. We propose

this is possible due to the greater amounts of ground ice build-up along the pole-facing scarp during periods of lower obliquity (25˚) and then sublimating during periods of high obliquity (45˚), resulting in a single step being created. The near-constant solar insolation along the equator-facing slope throughout the full range of obliquity periods results in ground ice continuously being sublimated, resulting in a much-gentler slope.

The craters we observed exhibiting scallops atop their ejecta blankets could be explained by aeolian processes removing the SDBT over time. The craters within the most-densely scalloped region exhibit much greater levels of erosion than the other locations, which can be explained by the greater aeolian processes occurring within the most-densely scalloped region. The potential scallops within the young crater ejecta in the eastern region (Figure 19) might also be explained by this, as well.

Topography and aeolian processes playing a role in scallop development is further demonstrated by the notable landforms observed in the higher latitudes of the study area (Figure 24). While the region is entirely devoid of scallops, these landforms exhibit "moats" around topographic obstacles such as mounds or craters. Combined with heavy dust devil activity within the region, suggesting concentrated aeolian activity, this demonstrates how wind could have carved these features over time. As stated earlier, these features are notable in that they initially have the appearance of scallops, but lack the steps used as the primary criteria for mapping scallops in this study.

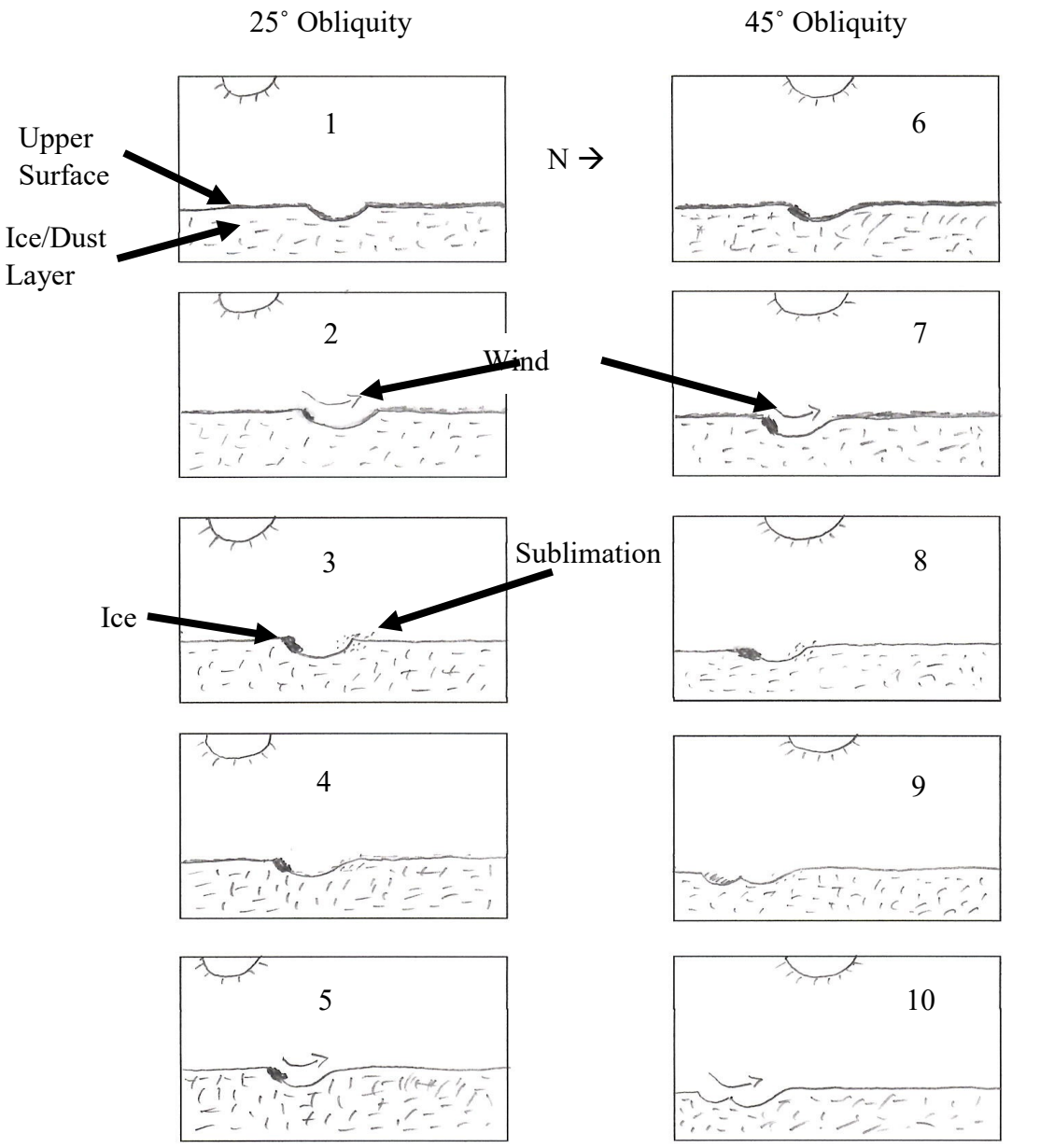

Figure 27: Conceptual model illustrating scalloped depression development during present obliquity (25˚) (left column), and development during periods of high obliquity (45˚) (right column).

The geomorphology of the scallops within the SHARAD reflector region could best be explained by variations in ice content within the landscape, rather than topographic effects, possibly attributing to the 50-85% water ice composition, as outlined in *Stuurman* et al. (2016). The greater water ice content and variations in directional growth might also indicate that these scallops formed at a greater range of obliquities. As noted above, *Lefort* et al. (2009) discuss how each step within a scallop could correspond to a different period of high obliquity, and that the presence of two or three interior ridges suggest that the formation of larger scallops has occurred over several obliquity cycles. While this might be likely for traditional scallops, we find this unlikely for the scallops within the SHARAD reflector region given how closely-spaced the steps are compared to traditional scallops within the study area.

Climate models from *Laskar* et al. (2004) suggest Mars has experienced multiple periods of high obliquity (≥45˚) between ~5 Ma and ~20 Ma, which is consistent with the assertion of previous studies that scalloped depressions first appeared in the Late Amazonian due to greater amounts of solar radiation along the pole-facing scarp during periods of high obliquity (e.g., *Sejourne* et al., 2011).

Chapter 4: Conclusion and Future Work

This research was undertaken to investigate the distribution and direction of growth of scalloped depressions in Utopia Planitia and to determine how topography might play a role in their development. Building upon previous studies into scalloped depressions in Utopia Planitia (e.g., *Kerrigan*, 2013; *Stuurman* et al., 2016; *Harrison* et al., 2019), we mapped the locations and growth direction of scalloped depressions residing within the study area, refined the map originally created by *Kerrigan* (2013), proposed a modification for the *Séjourné* et al. (2011) model for how topography and greater aeolian processes play a role in scalloped depression development, and identified how certain scallops within the study area could be explained by compositional variations.

Major Findings

The major finding of this research was that the most densely-scalloped region resides in a region of lower spatial density of craters previously mapped by *Harrison* et al. (2019) within a low-elevation region—although, not the lowest elevation—in Utopia Planitia. These scallops also proved to be the largest in the study area. We hypothesize that greater participation of aeolian processes potentially play a role in their development, as the sublimation lag was removed at a faster rate than in the rest of the study area, giving way to greater amounts of sublimation, and ultimately, larger scallops.

Secondly, the majority of scallops exhibiting more non-poleward azimuths (60˚-300˚) reside within the SHARAD reflector region, which is a region thought to have a composition of 50-85% water ice (*Stuurman*, 2016). This finding is important since this shows how composition, and not topography, may play a role in scallop development.

Research Questions

In summary, the questions proposed at the beginning of this research have been answered as followed:

1. What is the direction of growth of scalloped depressions within the mapped region?

A total of 93.9% of mapped scalloped depressions exhibit poleward-facing azimuths between 300˚-60˚, while the majority of remaining scallops exhibiting azimuths between 60˚-300˚ reside within the ice-rich region mapped by SHARAD.

2. How does topography affect scalloped depression growth and development?

We determined that topography appears to play a role in scallop development, as noted by the most-densely scalloped region residing within a topographic-low region where aeolian processes would be greater and temperatures higher due to a thicker atmosphere, resulting in larger scallops. Scallops were also observed atop crater ejecta outside of the most densely-scalloped region with the surrounding area almost entirely devoid of scallops. We also located potential scallops atop ejecta of the largest—and possibly youngest—crater in the eastern region of the study area. Landforms exhibiting moats around topographical obstacles such as raised crater rims within regions devoid of scallops—but experiencing heavy dust devil activity—also exhibited geomorphological similarities to scallops, but without steps.

3. What does this tell us about the geologic history of Utopia Planitia in the Amazonian?

With almost 94% of scallops demonstrating equatorward expansion, these findings are consistent with scallops having developed in the Late Amazonian when Mars was at high obliquity (~45˚) due to greater solar radiance along the pole-facing scarp.

Future Work

Numerous future studies into scalloped depressions can come from this work. The most notable is conducting a similar study into how topography affects scallop growth and development with scallops in the southern hemisphere, as scallops have already been observed and studied in the Peneus and Amphitrites regions, just south of Hellas Basin (*Lefort* et al., 2010 & *Zanetti* et al., 2010).

Given the observations made in scallops within the SHARAD reflector region, HiRISE and HiRISE DTM investigations similar to the *Lefort* et al. (2009) study could be conducted to better understand their morphology, although the lack of HiRISE DTMs in the region would make this study difficult at this time.

Further study into the potential scallops residing at the young crater in the eastern region could help determine how scalloped depressions develop over time, using the scallops found atop crater ejecta outside of the most-densely scalloped region as a reference point.

While briefly mentioned, the small, step-less scallops identified in the westernmost region of the study area could also be studied using HiRISE and HiRISE DTMs, but at present there are no such data sets available within that region of the study area. These scallops are intriguing since they don't appear to coalesce, as seen in the most-densely scalloped region.

REFERENCES

Christensen, P., Engle, E., Anwar, S., Dickenshied, S., Noss, D., Gorelick, N., & Weiss-Malik, M. (2009). *JMARS – A Planetary GIS*, **http://adsabs.harvard.edu/abs/2009AGUFMIN22A..06C**

Harrison, T. N. (2016). Martian Gully Formation and Evolution : Studies From the Local to Global Scale, (August).

Hauber, E., Reiss, D., & Ulrich, M. (2011). Landscape evolution in Martian mid-latitude regions : Insights from analogous periglacial landforms in Svalbard Landscape evolution in Martian mid-latitude regions : insights from analogous periglacial landforms in Svalbard. *Geological Society*, *356*(Special Publications), 111–131. https://doi.org/10.1144/SP356.7

Hudson, T. L., Aharonson, O., & Schorghofer, N. (2009). Laboratory experiments and models of diffusive emplacement of ground ice on Mars. *Journal of Geophysical Research*, *114*(E01002), 1–21. https://doi.org/10.1029/2008JE003149

Kerrigan, M. C., Osinski, G. R., Capitan, R. D., Barry, N., Blain, S., & Van De Wiel, M. J. (2012). The distribution and stratigraphy of periglacial landforms in western Utopia Planitia, Mars. *43rd Lunar and Planetary Science Conference*, 2716.

Kerrigan, M. C. (2013). The Periglacial Landscape Of Utopia Planitia ; Geologic Evidence For Recent Climate Change On Mars. *Master's Thesis, University of Western Ontario*.

Kreslavsky, M. A., & Head, J. W. (2003). North-south topographic slope asymmetry on Mars: Evidence for insolation-related erosion at high obliquity. *Geophysical Research Letters*, *30*(15), 1–4. https://doi.org/10.1029/2003GL017795

Gatto L. and Anderson D. (1975). Alaskan Thermokarst Terrain and Possible Martian Analog. *Science*, *188*(4185), 255–257.

Laskar, J., Correia, A. C. M., Gastineau, M., Joutel, F., Levrard, B., & Robutel, P. (2004). Long term evolution and chaotic diffusion of the insolation quantities of Mars. *Icarus*, *170*(2), 343–364. https://doi.org/10.1016/j.icarus.2004.04.005

Lefort, A., Russell, P. S., Thomas, N., McEwen, A. S., Dundas, C. M., & Kirk Physikalisches, R. L. (2009). Observations of periglacial landforms in utopia planitia with the high resolution imaging science experiment (HiRISE). *Journal of Geophysical Research E: Planets*, *114*(4), 1–18. https://doi.org/10.1029/2008JE003264

Lefort, A., Russell, P. S., & Thomas, N. (2010). Scalloped terrains in the Peneus and Amphitrites Paterae region of Mars as observed by HiRISE. *Icarus*, *205*(1), 259–268. https://doi.org/10.1016/j.icarus.2009.06.005

Levrard, Benjamin; Forget, Francois; Montmessin, Franck; Laskar, J. (2004). Recent ice-rich deposits formed at high latitudes on Mars by sublimation of unstable equatorial ice during low obliquity. *Nature*, *431*, 26–29. https://doi.org/10.1038/nature03006.1.

Levy, J., Head, J., & Marchant, D. (2009). Thermal contraction crack polygons on Mars : Classification , distribution , and climate implications from HiRISE observations. *Journal of Geophysical Research*, *114*(E01007), 1–19. https://doi.org/10.1029/2008JE003273

Madeleine, J. B., Forget, F., Head, J. W., Levrard, B., Montmessin, F., & Millour, E. (2009). Amazonian northern mid-latitude glaciation on Mars: A proposed climate scenario. *Icarus*, *203*(2), 390–405. https://doi.org/10.1016/j.icarus.2009.04.037

Mellon, Michael T; Jakosky, B. M. (1993). Geographic Variations in the Thermal and Diffusive Stability of Ground Ice on Mars. *Journal of Geophysical Research E: Planets*, *98*(E2), 3345–3364.

Mellon, M. T., & Jakosky, B. M. (1995). The distribution and behavior of Martian during past and present epochs. *Journal of Geophysical Research E: Planets*, *100*(E6), 11781–11799.

Morgenstern, A., Hauber, E., Reiss, D., van Gasselt, S., Grosse, G., & Schirrmeister, L. (2007). Deposition and degradation of a volatile-rich layer in Utopia Planitia and implications for climate history on Mars. *Journal of Geophysical Research E: Planets*, *112*(6), 1–11. https://doi.org/10.1029/2006JE002869

Plescia, J. B. (2003). Cerberus Fossae , Elysium , Mars : a source for lava and water. *Icarus*, *164*, 79–95. https://doi.org/10.1016/S0019-1035(03)00139-8

Schorghofer, N., & Aharonson, O. (2005). Stability and exchange of subsurface ice on Mars. *Journal of Geophysical Research*, *110*(E05003), 1–16. https://doi.org/10.1029/2004JE002350

Schorghofer, N. (2007). Dynamics of ice ages on Mars. *Nature*, *449*, 192–195. https://doi.org/10.1038/nature06082

Schorghofer, N., & Forget, F. (2012). History and anatomy of subsurface ice on Mars. *Icarus*, *220*(2), 1112–1120. https://doi.org/10.1016/j.icarus.2012.07.003

Séjourné, A., Costard, F., Gargani, J., Soare, R. J., Fedorov, A., & Marmo, C. (2011). Scalloped depressions and small-sized polygons in western Utopia Planitia, Mars: A new formation hypothesis. *Planetary and Space Science*, *59*(5–6), 412–422. https://doi.org/10.1016/j.pss.2011.01.007

Séjourné, A., Costard, F., Gargani, J., Soare, R. J., & Marmo, C. (2012). Evidence of an eolian ice-rich and stratified permafrost in Utopia Planitia, Mars. *Planetary and Space Science*, *60*(1), 248–254. https://doi.org/10.1016/j.pss.2011.09.004

Sharp, R. P. (1973). Mars : Fretted and Chaotic Terrains possible genesis of these two terrain types . More will undoubtedly be written about them as the with only a minor extension south of the equator . Other areas of fretted terrain may exist , but they ranging as far west. *Journal of Geophysical Research*, *78*(20), 4073–4083.

Soare, R. J., Osinski, G. R., & Roehm, C. L. (2008). Thermokarst lakes and ponds on Mars in the very recent (late Amazonian) past. *Earth and Planetary Science Letters*, *272*(1–2), 382–393. https://doi.org/10.1016/j.epsl.2008.05.010

Soare, R. J., Horgan, B., Conway, S. J., Souness, C., & El-Maarry, M. R. (2015). Volcanic terrain and the possible periglacial formation of "excess ice" at the mid-latitudes of Utopia Planitia, Mars. *Earth and Planetary Science Letters*, *423*, 182–192. https://doi.org/10.1016/j.epsl.2015.04.033

Stuurman, C. M., Osinski, G. R., Holt, J. W., Levy, J. S., Brothers, T. C., Kerrigan, M., & Campbell, B. A. (2016). SHARAD detection and characterization of subsurface water ice deposits in Utopia Planitia, Mars. *Geophysical Research Letters*, *43*(18), 9484–9491. https://doi.org/10.1002/2016GL070138

Ulrich, M., Morgenstern, A., Günther, F., Reiss, D., Bauch, K. E., Hauber, E., … Schirrmeister, L. (2010). Thermokarst in Siberian ice - rich permafrost : Comparison to asymmetric scalloped depressions on Mars. *Journal of Geophysical Research*, *115*(E10009), 1–22. https://doi.org/10.1029/2010JE003640

Zanetti, M., Hiesinger, H., Reiss, D., Hauber, E., & Neukum, G. (2010). Distribution and evolution of scalloped terrain in the southern hemisphere , Mars. *Icarus*, *206*(2), 691–706. https://doi.org/10.1016/j.icarus.2009.09.010

Zanetti, M., Hiesinger, H., Reiss, D., Hauber, E., & Münster, W. W. (2008). Scalloped Depression Development on Malea Planum and the Southern Wall of the. *40th Lunar and Planetary Science Conference*, *Abstract 2*.